



Burial and exhumation of Corsica (France) in the light of fission track data

Martin Danišik,¹ Joachim Kuhlemann,¹ István Dunkl,² Balázs Székely,¹
and Wolfgang Frisch¹

Received 19 December 2005; revised 6 July 2006; accepted 17 October 2006; published 4 January 2007.

[1] The Mesozoic and Cenozoic exhumation and cooling history of Corsica is reconstructed by fission track (FT) data on basement and sedimentary rocks. Apatite ages are 105–16 Ma; zircon ages are 160–145 Ma. The Jurassic and Cretaceous ages show that parts of the Variscan basement escaped Alpine influence. The basement was thermally affected by rifting prior to Jurassic opening of the Ligurian-Piedmont Ocean; then it cooled to near-surface temperatures. In Paleocene-Eocene times, subduction buried parts of the basement and overlying flysch to greater depth. In the Oligocene, both collapse of the nappe stack and rifting prior to opening of the Ligurian-Provençal Basin affected the apatite FT system of the basement in different, partly overlapping areas causing a complex age pattern. The study shows that thorough analysis of FT data and thermal modeling allow to assign age populations to distinct cooling processes even when several thermotectonic events contributed to generate an intricate age pattern. **Citation:** Danišik, M., J. Kuhlemann, I. Dunkl, B. Székely, and W. Frisch (2007), Burial and exhumation of Corsica (France) in the light of fission track data, *Tectonics*, 26, TC1001, doi:10.1029/2005TC001938.

1. Introduction

[2] The island of Corsica in the western Mediterranean represents the northern part of an isolated continental fragment (Corsica-Sardinia block) that is flanked by two oceanic basins (Figure 1). Since Corsica records both Alpine collisional evolution and subsequent postorogenic extension, it provides a unique opportunity to investigate the thermal response of continental crust to orogenic collision and postorogenic collapse. In this context, fission track (FT) thermochronology is particularly useful since it has become a well-established technique with the ability to provide thermal information over the temperature range characteristic of the uppermost kilometers of the crust. There are several advantageous features that make Corsica an excellent study area. For instance, the geological setting

is relatively simple: there are two major domains encountered on a relatively small territory, the succession of the major tectonic events is rather well established, and there are sufficient occurrences of sedimentary rocks that serve as important stratigraphic markers.

[3] Despite relatively intensive research in Corsica in the last decades on subjects such as the kinematics of the Alpine collision [e.g., *Mattauer et al.*, 1981; *Malavieille*, 1983; *Durand-Delga*, 1984; *Warburton*, 1986; *Malavieille et al.*, 1998], extension, inversion of the orogenic front, basin formation [e.g., *Fournier et al.*, 1991; *Jolivet et al.*, 1991; *Jolivet and Faccenna*, 2000], rotation of the Corsica-Sardinia block [e.g., *Vigliotti and Kent*, 1990; *Vigliotti et al.*, 1990; *Vigliotti and Langenheim*, 1995], or the high-pressure/low-temperature metamorphism event [e.g., *Caron et al.*, 1981; *Gibbons and Horák*, 1984; *Lahondère*, 1988; *Lahondère and Guerrot*, 1997], the issue of the low-temperature thermal evolution has not yet been adequately resolved. In fact, there have been numerous low-temperature geochronological studies carried out in Corsica, reporting entirely Cenozoic cooling ages that were interpreted in different ways. Although a relatively large database of FT data exists, the data are restricted mostly to the northeastern part [*Carpéna et al.*, 1979; *Lucazeau and Mailhé*, 1986; *Mailhé et al.*, 1986; *Cavazza et al.*, 2001; *Fellin*, 2003; *Fellin et al.*, 2005a] and the western coast of Corsica [*Lucazeau and Mailhé*, 1986; *Mailhé et al.*, 1986; *Jakni*, 2000; *Jakni et al.*, 2000; *Zarki-Jakni et al.*, 2004], whereas the central and southern parts remained virtually unexplored. Therefore our thermochronological study concentrates on these parts of the island.

[4] Our new data measured on basement and, more importantly, on sedimentary rocks allow us to identify previously unrecognized features and cooling events. Among others, for the first time the Mesozoic thermal evolution of Corsica is revealed by our apatite FT data. Further, we propose a new geodynamic model for Corsica, which emphasizes an important impact of sedimentary burial on the low-temperature history of the Variscan crustal fragments. Last but not least, our new model allows us to explain several contradictions published in other Corsican FT papers. We believe that this study helps to improve our understanding of the geodynamic and thermotectonic evolution of Corsica and the western Mediterranean in general.

2. Geological Setting and Tectonic Evolution

[5] Two distinct geological domains characterize the island of Corsica-Variscan and Alpine Corsica (Figure 2)

¹Institute of Geosciences, University of Tübingen, Tübingen, Germany.

²Geoscience Center Göttingen, Sedimentology and Environmental Geology, Göttingen, Germany.

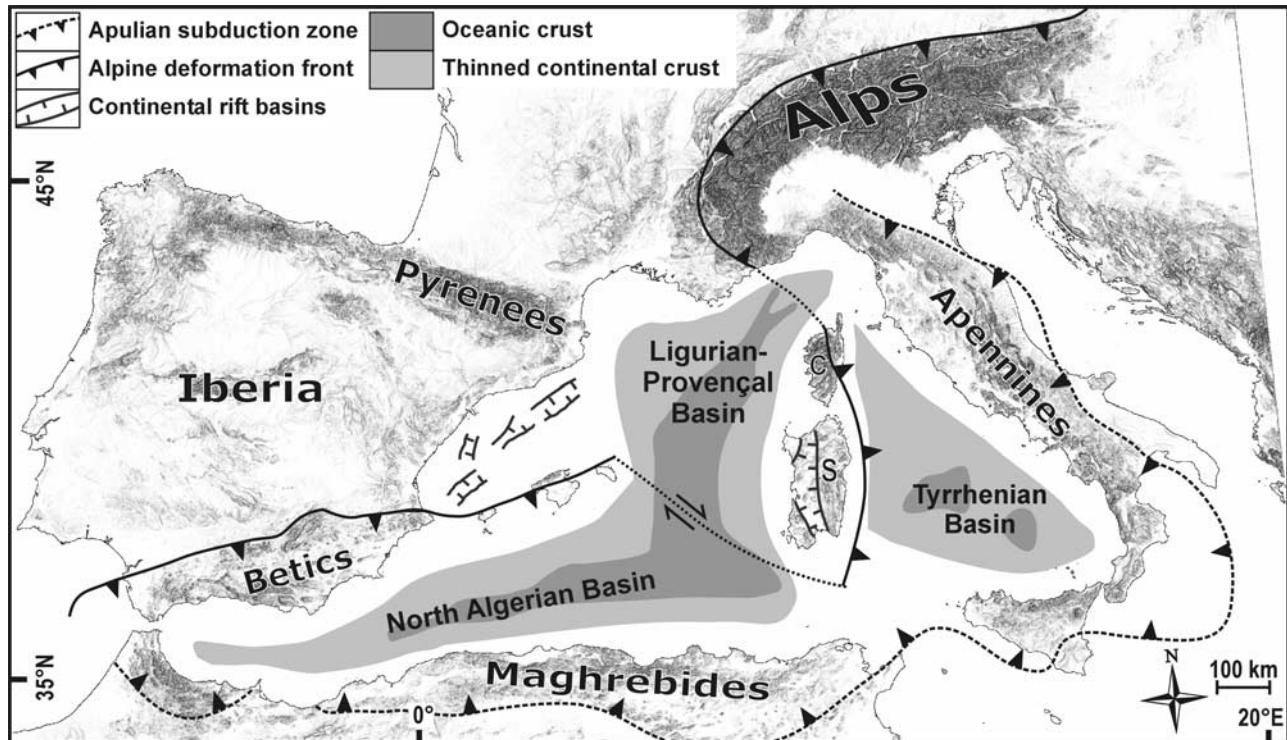


Figure 1. Digital elevation model of the western Mediterranean region with simplified major geological structures [after *Gueguen et al.*, 1998]. C, Corsica; S, Sardinia.

[*Durand-Delga*, 1978]. Variscan Corsica is a crystalline basement mostly built up of various granitoid and volcanic rocks with intrusion ages between 340 and 260 Ma, related to the Variscan orogeny and post-Variscan extension [*Cocherie et al.*, 1984; *Durand-Delga*, 1984; *Rossi and Cocherie*, 1991]. The igneous succession formed in two cycles: (1) synorogenic magmatism with calc-alkaline affinity during the Carboniferous and (2) postorogenic magmatism with alkaline affinity during the Permian [e.g., *Rossi et al.*, 1980].

[6] In the Mesozoic, the Variscan basement of the Corsica-Sardinia block was part of the south margin of the Laurasian plate. In Jurassic times, an extensional regime induced rifting and subsequent opening of the Ligurian-Piedmont Ocean that hosted oceanic crust and deep-sea sediments of later Alpine nappes, which represents the southern continuation of the western Alps [*Frisch*, 1981; *Loup*, 1992; *Borel*, 1995]. Oceanic spreading continued in Cretaceous times until subduction accounted for overall convergence [*Dewey et al.*, 1989]. The Ligurian-Piedmont Ocean was closed and the European plate margin became subducted toward the southeast under the African, or rather Apulian plate. The convergence resulted in the emplacement of nappes derived from the Ligurian-Piedmont Ocean and the distal European margin onto the Variscan basement of Corsica. Oceanic nappes and fragments of the continental margin of the European plate with their sedimentary cover (e.g., Tenda Massif, Corte slices) became metamorphosed during the Alpine orogeny partly under middle-pressure/

low-temperature (MP/LT) and partly under high-pressure/low-temperature (HP/LT) conditions [e.g., *Nardi et al.*, 1978; *Caron et al.*, 1981; *Mattauer et al.*, 1981; *Gibbons and Horák*, 1984; *Warburton*, 1986; *Jourdan*, 1988; *Daniel et al.*, 1996; *Malavieille et al.*, 1998]. The age of the metamorphism is still a matter of debate. Whereas *Malavieille et al.* [1998] favor a Late Cretaceous age of HP/LT event, *Brunet et al.* [2000] argue for an Eocene age. The youngest sediments affected by metamorphic overprint are mid-Eocene flysch sediments that were deposited in the trough in front of the approaching Alpine nappes during Alpine collision [*Durand-Delga*, 1978; *Egal*, 1992]. This flysch is composed of conglomerates with components from the Variscan basement, quartzites, arkoses, and pelites; its actual thickness is up to several hundreds of meters. In the late Eocene/early Oligocene, the compressional tectonic regime in Corsica changed to an extensional one due to the formation of the northwestward dipping, eastward retreating Apenninic subduction zone [e.g., *Réhault et al.*, 1984; *Doglionni*, 1991; *Gueguen et al.*, 1998]. Main Alpine thrust planes were reactivated as ductile normal faults by this time, leading to the collapse in the wedge and exhumation of metamorphosed units [*Réhault et al.*, 1984; *Jolivet et al.*, 1990, 1991, 1998; *Fournier et al.*, 1991; *Brunet et al.*, 2000].

[7] At ~30 Ma, continental rifting in the present-day Gulf of Lion started, subsequently leading to the opening of the Ligurian-Provençal Basin and separation of the Corsica-Sardinia block from the European mainland [*Bellaiche et*

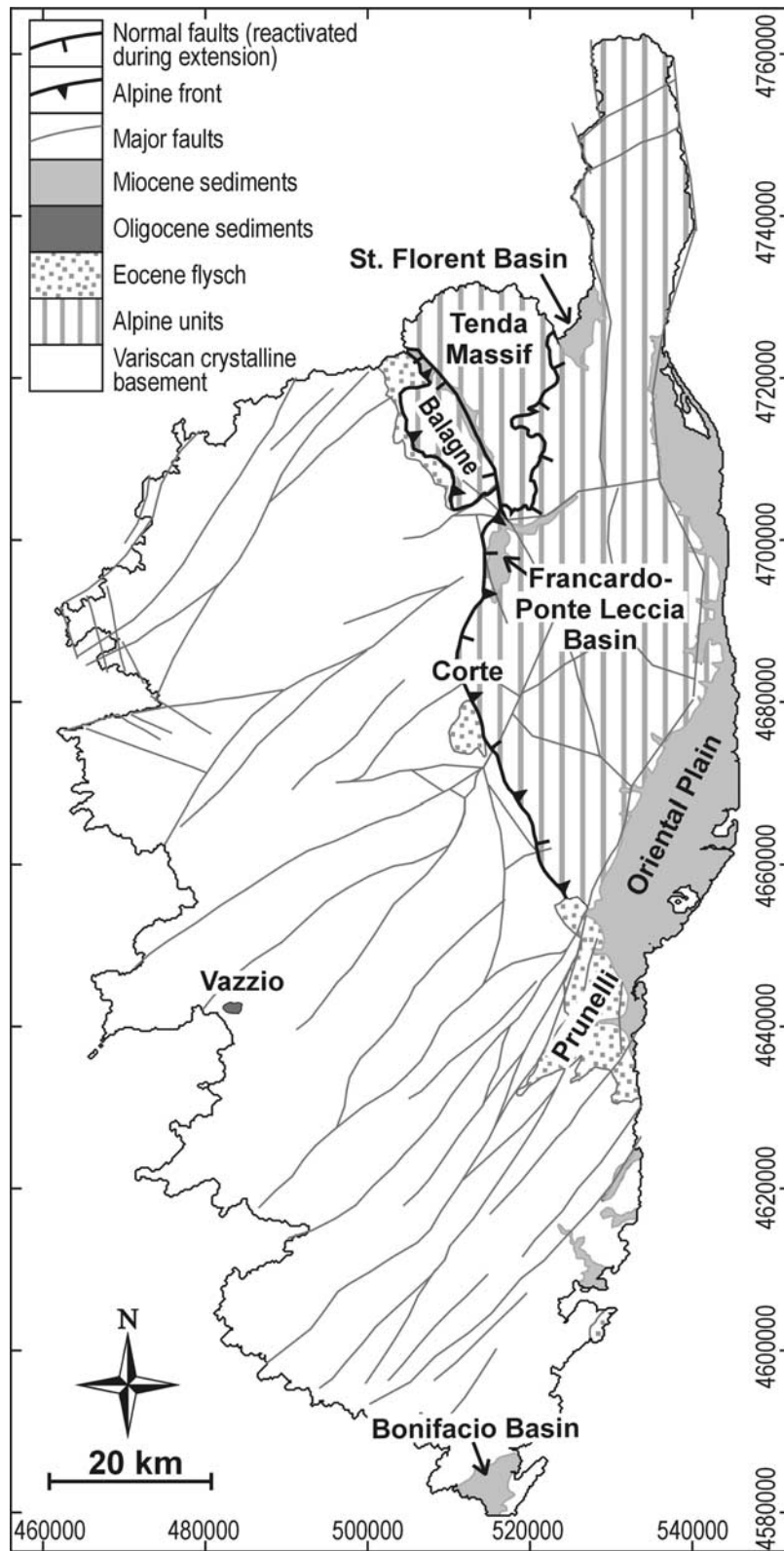


Figure 2. Schematic map of major lithotectonic units in Corsica [after Rossi et al., 1980].

al., 1976; *Cherchi and Montadert*, 1982; *Sérrane*, 1999]. First postcollisional deposits formed in the late Oligocene at the WSW coast. Fluvial coarse conglomerates from local basement sources, testifying steep local relief, were deposited in a half graben structure, which formed at the eastern shoulder of the Ligurian-Provençal rift system [*Ferrandini et al.*, 1999]. During the early Miocene (~21–17 Ma), the Corsica-Sardinia block rotated counterclockwise close to its present position, and oceanic crust formed in the Ligurian-Provençal Basin [*Vigliotti and Kent*, 1990; *Vigliotti et al.*, 1990; *Vigliotti and Langenheim*, 1995]. At ~18 Ma, rifting of the Tyrrhenian Basin started on the eastern side of Corsica [*Carmignani et al.*, 1995] followed by the formation of oceanic crust due to subduction rollback in the Apennines. This process left the Corsica-Sardinia block as a lithospheric boudin, flanked by two back-arc basins with respect to the westward dipping Apenninic subduction zone [*Dogliani et al.*, 1999; *Zeck*, 1999]. Between 17 and 10 Ma, extension and subsidence in eastern Corsica caused basin formation (see Figure 2) and transgressive deposition of terrestrial conglomerates, grading into carbonate-dominated, shallow marine deposits [*Orszag-Sperber and Pilot*, 1976; *Durand-Delga*, 1978]. Extension is attributed to the eastward retreat of the Apenninic subduction zone [e.g., *Dogliani et al.*, 1999]. Except for the eastern margin of the Oriental Plain, deposition in the Miocene basins terminated by ~10 Ma [*Durand-Delga*, 1978], and facies of fluvial conglomerates of the youngest deposits record uplift and increase of relief in the hinterland by this time [*Ferrandini et al.*, 1998].

3. Available Geochronologic and Stratigraphic Constraints

[8] An important constraint on the age of HP/LT metamorphism was provided by *Lahondère and Guerrot* [1997], who reported a Sm/Nd age of 83.8 ± 4.9 Ma (isochron defined on a whole rock-garnet-glaucophane-clinopyroxene assemblage) from an eclogitic lens in gneissic rocks in Alpine Corsica (for location, see Figure 3a), pointing to a Cretaceous age of HP metamorphism in the Alpine nappes.

[9] A large number of $^{40}\text{Ar}/^{39}\text{Ar}$ mica ages is reported from NE Corsica [*Maluski*, 1977; *Amaudric du Chaffaut and Saliot*, 1979; *Mailhé*, 1982; *Jourdan*, 1988; *Lahondère*, 1991; *Brunet et al.*, 1997; *Brunet et al.*, 2000]. They range between ~65 and 25 Ma. A summarizing interpretation was presented by *Brunet et al.* [2000], who argued that thrusting of the Alpine nappes onto the Variscan basement lasted from ~45 to 32 Ma. Inversion of shear sense and reactivation of thrust planes as extensional shear zones resulted in the tectonic denudation of metamorphic rocks between 33 and 25 Ma.

[10] The pioneering zircon FT ages (ZFT) from Corsica were presented by *Carpéna et al.* [1979] and *Mailhé et al.* [1986]. However, in these studies, the ZFT results were not considered by other authors [see *Cavazza et al.*, 2001; *Fellin*, 2003; *Zarki-Jakni et al.*, 2004; *Fellin et al.*, 2005a] although the veracity of these data has never been disproved. The ZFT ages range between 225 and 36 Ma and

show a clear trend of decreasing ages from west to east. This is interpreted by the authors as partial resetting of Variscan ages according to the varying overburden of the Alpine nappe pile during collision. More recently, some additional ZFT ages (74, 69, 21, 19 Ma, no errors given) were reported from Alpine Corsica [*Zattin et al.*, 2001; *Fellin et al.*, 2005a], providing additional constraints on the cooling history.

[11] A number of apatite FT (AFT) data has been published from Corsica [*Carpéna et al.*, 1979; *Lucazeau and Mailhé*, 1986; *Mailhé et al.*, 1986; *Cavazza et al.*, 2001; *Fellin*, 2003; *Jakni*, 2000; *Jakni et al.*, 2000; *Zarki-Jakni et al.*, 2004; *Fellin et al.*, 2005a]. However, not all these reports are provided with sufficient information. Older studies [*Carpéna et al.*, 1979; *Lucazeau and Mailhé*, 1986; *Mailhé et al.*, 1986], based on the population dating method, reported AFT ages, which were older than the $^{40}\text{Ar}/^{39}\text{Ar}$ white mica and zircon fission track ages from the same location. Moreover, these studies do not present track length data, which is crucial for meaningful interpretation of AFT results. In recent studies, these data were considered to be inaccurate and therefore ignored (for details, see discussions by *Cavazza et al.* [2001] and *Zarki-Jakni et al.* [2004]). We follow this decision and also do not take into account these early AFT data in our study.

[12] Several recent studies [*Jakni*, 2000; *Jakni et al.*, 2000; *Cavazza et al.*, 2001; *Fellin*, 2003; *Zarki-Jakni et al.*, 2004; *Fellin et al.*, 2005a], based on the external detector dating method, report substantially younger AFT ages, which are in line with the cooling history yielded by the higher temperature thermochronometers. Therefore we try to integrate these data into our results. However, even these recent studies do not always provide necessary information such as accurate sample coordinates and laboratory procedures used, or they provide statistically inadequate results (e.g., too few grains are counted). Consequently, the data of different studies are often contradictory, and the integration of different data sets and compilation of a robust database is complicated. Therefore the data require some critical evaluation as described in section 6.2.1.

[13] *Cavazza et al.* [2001] present AFT data from an E-W oriented profile crossing the Alpine and Variscan domains in the NE part of the island. The ages range from 19.6 ± 3.5 to 13.8 ± 0.16 Ma. The data record an episode of exhumation during early to middle Miocene times. There are no systematic differences in age between the structural units. This implies synchronous Neogene exhumation and absence of significant differential vertical displacement between footwall (Variscan Corsica) and hanging wall (Alpine Corsica) or between individual nappes. Because of the complete resetting of the ages of Eocene foreland sedimentary samples, *Cavazza et al.* proposed that prior to Miocene exhumation, the area was covered by higher nappes or neoautochthonous sediments.

[14] Studies of *Jakni* [2000], *Jakni et al.* [2000], and *Zarki-Jakni et al.* [2004] report AFT data both from Alpine and Variscan Corsica. The AFT cooling ages from Alpine Corsica range from 22.5 ± 1.2 to 12.3 ± 2.9 Ma and are consistent with those of *Cavazza et al.* [2001]. From

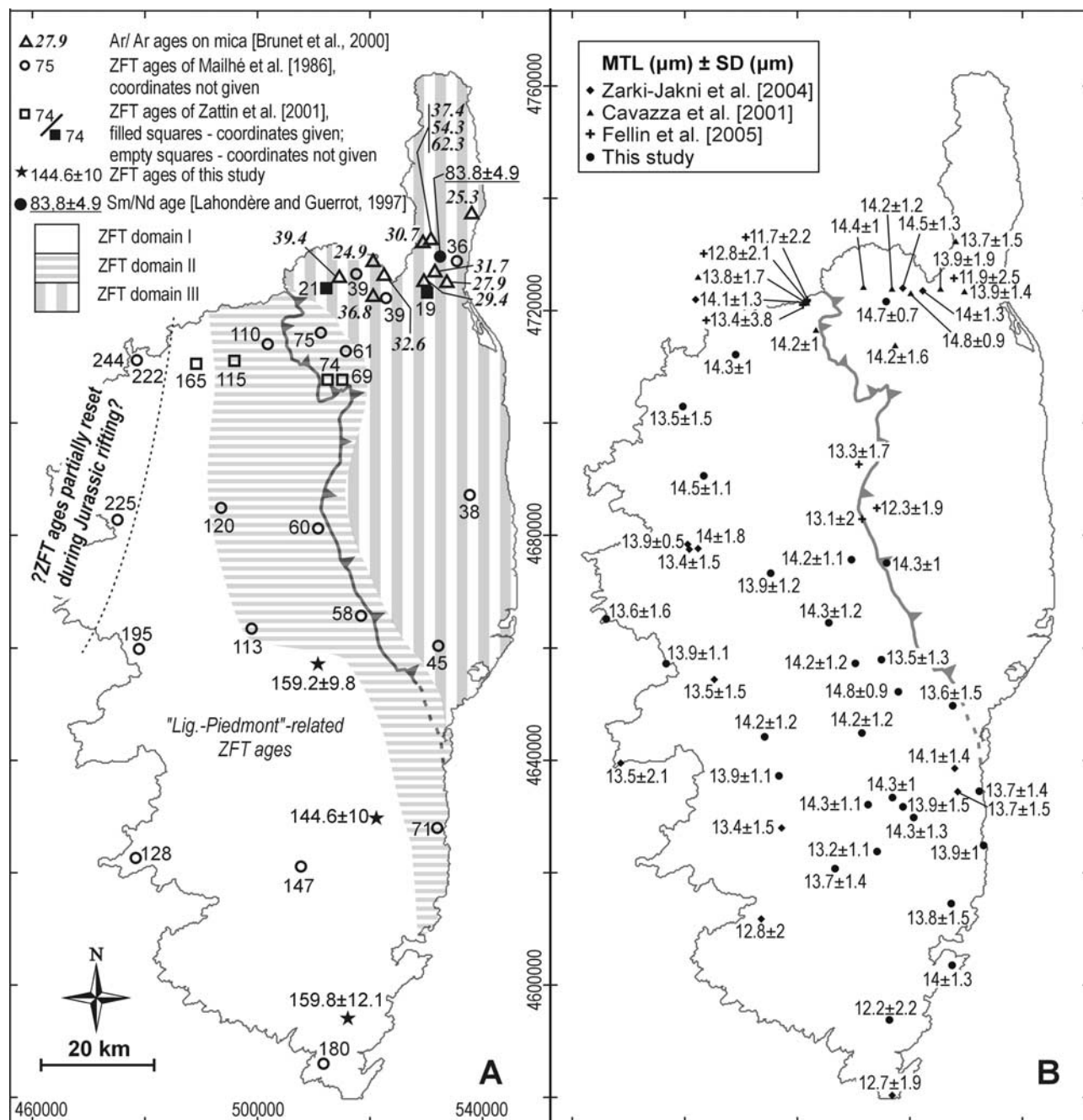


Figure 3. (a) Distribution of ZFT, $^{40}\text{Ar}/^{39}\text{Ar}$ and Sm/Nd data and subdivision of Corsica into ZFT domains (see text for explanation). (b) Track length data expressed by mean track length and standard deviation. Standard errors are not shown.

Variscan Corsica, a relatively wide AFT age variation from 53.8 ± 4.1 to 10.5 ± 0.8 Ma is presented, which, according to the authors, form a clear spatial pattern: AFT ages >30 Ma show broad track length distributions and occur in the SW part of the island. AFT ages <30 Ma with narrow track length distributions form a crescent-shaped pattern running from the NW to the SE, where ages become younger with decreasing distance to the Alpine thrust front. The ages from the west and NW coast are interpreted to record cooling

related to erosional denudation, which is attributed to the rifting in the area of the later Ligurian-Provençal and passive margin uplift. The younger ages close to the Alpine front are interpreted as recording cooling related to eastward migration of extension from the Ligurian-Provençal Basin to the Tyrrhenian Basin.

[15] Studies of Fellin [2003] and Fellin et al. [2005a] report AFT data in range of 30.5 ± 3.2 to 12.7 ± 2 Ma. They present detailed structural and sedimentological analyses

Table 1. Zircon Fission Track Data^a

Sample Code	UTM32/WGS84		Altitude, m	Tectonic Unit	Petrography	N	ρ_s	N_s	ρ_i	N_i	ρ_d	N_d	P(χ^2), %	Age, Ma	$\pm 1\sigma$, Ma
	X	Y													
KU-22	515936	4593844	876	Variscan basement	granite	20	161.360	1163	34.825	251	5.637	2675	51.5	159.8	12.1
XC-46	510622	4656974	2247	Variscan basement	granite	25	193.548	1860	41.727	401	5.609	2675	100.0	159.2	9.8
XC-50	521008	4629515	500	Variscan basement	granite	25	59.364	1295	14.073	307	5.595	2675	100.0	144.6	10

^aN is number of dated apatite crystals; ρ_s (ρ_i) are spontaneous (induced) track densities ($\times 10^5$ tracks/cm²); N_s (N_i), is number of counted spontaneous (induced) tracks; ρ_d is dosimeter track density ($\times 10^5$ tracks/cm²); N_d is number of tracks counted on dosimeter; P(χ^2) is probability obtaining chi-square value (χ^2) for n degree of freedom (where n is number of crystals minus 1); age $\pm 1\sigma$ is central age ± 1 standard error [Galbraith and Laslett, 1993]. Ages were calculated using zeta calibration method [Hurford and Green, 1983], glass dosimeter CN-2, and zeta value of 123.92 ± 2.53 yr/cm².

from the Miocene basins of central and NE Corsica. The results indicate rapid cooling related to exhumation of the pre-Neogene basement (Variscan and Alpine units) during the early to middle Miocene. The exhumation was accompanied by normal faulting, leading to subsidence and formation of a narrow basin in central and eastern Corsica since the Burdigalian. This basin was inverted during the Tortonian in the course of final exhumation.

4. Methods and Analytical Procedure

4.1. Dating Method

[16] Fission tracks are linear trails of damage in the crystal lattice produced by the spontaneous fission of ²³⁸U and form continuously through time [Wagner, 1968]. At high temperatures (in case of apatite above $\sim 120^\circ\text{C}$, in case of zircons above $\sim 300^\circ\text{C}$) fission tracks are annealed in a short time. When a rock cools to a certain temperature range (the so-called partial annealing zone, PAZ), retention of the fission tracks starts. For apatite, the PAZ is generally defined as a temperature range between $\sim 60^\circ\text{C}$ and 120°C (referred to as APAZ), for zircon between $\sim 200^\circ\text{C}$ and 300°C (referred to as ZPAZ) [see e.g., Wagner and Van den haute, 1992]. Within the PAZ, the fission tracks are progressively shortened, depending on the temperature and time spent in the PAZ. By using fission track length distributions it is therefore possible to investigate the thermal history of the rocks and model the time-temperature trajectory of a sample [Gleadow et al., 1986a, 1986b; Yamada et al., 1995].

4.2. Sampling and Analytical Procedure

[17] We focused our sampling campaign primarily on Variscan Corsica, particularly on those regions, from where no AFT ages had been reported. Series of samples were taken from the Eocene flysch along the Alpine deformation front to investigate possible resetting of AFT ages in these sediments. Elevation profiles in steep relief regions from homogeneous blocks without internal faulting were sampled in order to evaluate exhumation rates. Some additional samples were taken from Alpine Corsica. A total of 157 samples of granitoids, gneisses, sandstones and conglomerates was collected, however many lithologies were surprisingly poor in apatite, thus only 67 out of the set contained sufficient amounts of datable apatite crystals.

[18] For FT analysis the external detector method [Gleadow, 1981] was used. FT ages were calculated using the ζ (zeta) age calibration method [Hurford and Green, 1983]. Modeling of the low-temperature thermal history based on AFT data was carried out using the HeFTy modeling program [Ketchum, 2005]. The annealing kinetics of apatite fission tracks was assessed by measurement of Dpar values (Dpar is the etch pit diameter of fission tracks parallel to the crystallographic c axis at the polished, etched, and analyzed apatite surface) [Crowley et al., 1991; Naeser, 1992; Burtner et al., 1994]. A detailed description of the analytical procedure used can be found in Appendix A.

5. Results

5.1. Zircon Fission Track Ages

[19] ZFT ages were measured on three samples from the southern and central part of the Variscan granitic basement in order to verify accuracy of the data presented in previous studies (Table 1 and Figure 4). All samples passed the chi-square test at a 95% confidence interval and are reported as central ages with ± 1 sigma errors. The ZFT ages are 159.8 ± 12.1 (KU-22), 159.2 ± 9.8 (XC-46) and 144.6 ± 10 Ma (XC-50) and thus younger than the intrusion ages of the granites (~ 340 – 260 Ma [Cocherie et al., 1984]).

5.2. Apatite Fission Track Ages

[20] AFT analyses were performed on 67 samples (Table 2 and Figure 4). All samples passed the chi-square test at the 95% confidence interval and are reported as central ages with ± 1 sigma errors. The AFT ages from granites in Variscan Corsica are considerably younger than the intrusion ages. All but two ages are Cenozoic, ranging from 46.4 ± 4 (XC-81) to 16.4 ± 1.4 Ma (XC-116). Samples XC-2 and KU-22 from southernmost Corsica are Cretaceous (105.3 ± 7.2 and 97.9 ± 5.4 Ma, respectively). The AFT ages from the Eocene flysch are all younger than the depositional ages (~ 60 – 40 Ma, upper Paleocene to middle Eocene [Durand-Delga, 1978; Rossi et al., 1980]) and range from 30.6 ± 1.6 (XC-85) to 16.4 ± 1 Ma (XC-132). Samples from the Tenda Massif (basement complex metamorphosed during Alpine orogeny) yielded AFT ages in the range of 24.9 ± 2.7 (XC-42) to 16.4 ± 1.4 Ma (XC-116).

Table 2. Apatite Fission Track Data^a

Sample Code	UTM32/WGS84		Altitude, m	Tectonic Unit	Petrography	N	ρ_s	N_s	ρ_i	N_i	ρ_d	N_d	P(χ^2), %	Age, Ma	$\pm 1\sigma$, Ma	MTL, μm	SD, μm	SE, μm	N (L)	Dpar, μm
	X	Y																		
XC-2	516683	4593456	280	Variscan basement	granite	25	12.842	564	11.453	503	5.575	4936	99.9	105.3	7.2	12.2	2.2	0.2	101	1.61
XC-6	514493	4623457	826	Variscan basement	granite	25	5.403	297	17.301	951	5.312	4936	100.0	28.1	2.1	13.2	1.1	0.1	95	1.79
XC-12	489324	4711884	550	Variscan basement	granite	25	4.268	338	16.783	1329	5.400	4936	100.0	23.3	1.6	14.3	1.0	0.1	100	1.52
XC-17	504586	4684921	1758	Variscan basement	granite	25	1.579	125	7.375	584	7.780	5426	99.9	27.4	2.8					3.24
XC-22	476440	4678574	60	Variscan basement	granite	25	5.761	413	28.302	2029	6.149	5647	99.5	20.8	1.2					3.48
XC-27	509772	4649947	1754	Variscan basement	granite	25	3.281	263	11.279	904	6.194	5647	100.0	29.9	2.2					3.86
XC-29	509206	4635978	940	Variscan basement	granite	26	3.422	272	15.011	1193	6.326	5647	100.0	23.9	1.7	14.2	1.2	0.1	98	2.27
XC-31	511783	4644575	800	Variscan basement	granite	25	2.497	155	7.877	489	5.487	4936	100.0	29.5	2.9					1.59
XC-32	515893	4649042	1065	Variscan basement	granite	25	2.992	243	12.906	1048	7.341	5426	86.7	28.0	2.1					3.78
XC-33	518273	4651914	1874	Variscan basement	granite	25	3.261	152	12.230	570	5.429	4936	100.0	24.5	2.4	14.8	0.9	0.1	85	1.68
XC-34	515262	4657639	800	Variscan basement	granite	27	3.026	164	16.328	885	5.796	5647	99.9	17.8	1.6	13.5	1.3	0.2	52	1.71
XC-39	483649	4690293	200	Variscan basement	granite	50	4.962	545	25.209	2769	5.283	4936	100.0	17.6	1.0	14.5	1.1	0.1	80	1.56
XC-41	508911	4691175	463	Variscan basement	granite	25	1.396	117	7.423	622	7.466	5426	85.1	23.1	2.4					1.60
XC-42	516582	4703360	230	Tenda Massif	orthogneiss	34	2.009	117	7.470	435	5.458	4936	100.0	24.9	2.7					1.50
XC-46	510622	4656974	2247	Variscan basement	granite	36	1.006	112	4.022	448	5.517	4936	100.0	23.4	2.6	14.2	1.2	0.1	65	1.63
XC-48	514759	4611153	1095	Variscan basement	granite	25	1.723	148	6.262	538	7.655	5426	98.6	34.6	3.3					3.29
XC-50	521008	4629515	500	Variscan basement	granite	25	3.896	234	9.091	546	5.195	4936	100.0	37.7	3.2	14.3	1.3	0.1	90	1.89
XC-54	507010	4620408	321	Variscan basement	granite	25	7.804	291	22.072	823	5.953	5647	100.0	34.9	2.5	13.7	1.4	0.1	91	1.80
XC-59	516108	4721345	520	Tenda Massif	orthogneiss	30	4.590	251	21.488	1175	5.663	4936	100.0	20.5	1.6	14.7	0.7	0.1	81	1.59
XC-63	508011	4664924	2295	Variscan basement	granite	25	2.462	317	12.922	1664	6.839	5426	99.1	21.4	1.4					1.67
XC-64	507556	4663280	1410	Variscan basement	granite	25	1.732	248	9.826	1407	7.153	5426	99.7	20.8	1.5					1.63
XC-67	494484	4643898	200	Variscan basement	granite	25	3.357	241	12.175	874	6.643	5647	100.0	30.4	2.3	14.2	1.2	0.1	71	1.92
XC-69	500065	4646344	750	Variscan basement	granite	25	3.312	338	10.082	1029	6.964	5426	99.7	37.6	2.5					3.13
XC-74	512890	4631804	1627	Variscan basement	granite	25	3.007	352	13.276	1554	6.538	5647	97.8	24.6	1.6	14.3	1.1	0.2	43	1.66
XC-75	517225	4633070	2133	Variscan basement	granite	25	2.912	230	10.013	791	5.902	5647	100.0	28.5	2.3	14.3	1.0	0.1	46	1.79
XC-76	518153	4643651	1981	Variscan basement	granite	25	2.169	236	8.374	911	6.901	5426	100.0	29.4	2.3					1.73
XC-77	521458	4645523	530	Variscan basement	granite	25	1.463	177	6.620	801	5.781	5426	99.2	21.0	1.8					1.70
XC-78	521695	4640541	325	Variscan basement	granite	25	1.806	139	9.198	708	6.573	5647	100.0	21.4	2.1					2.25
XC-81	511052	4600940	300	Variscan basement	granite	25	2.630	206	7.010	549	7.529	5426	97.6	46.4	4.0					3.17
XC-85	519102	4631419	1880	Eocene flysch	arkose	35	5.379	581	19.404	2096	6.661	5647	99.9	30.6	1.6	13.9	1.5	0.2	81	1.66
XC-86	523445	4625414	1040	Variscan basement	granite	31	4.031	368	14.524	1326	6.785	5647	100.0	31.2	2.0					1.57
XC-87	505553	4678052	1033	Variscan basement	granite	25	1.338	148	7.097	785	7.215	5426	99.4	22.4	2.1					4.50
XC-88	505491	4674372	2404	Variscan basement	granite	30	1.686	169	7.173	719	6.080	5647	100.0	23.7	2.1					2.11
XC-89	504767	4673776	2620	Variscan basement	granite	25	2.475	205	12.641	871	6.838	5647	100.0	26.7	2.2					2.77
XC-90	509929	4675353	2453	Eocene flysch	arkose	25	4.446	232	20.716	1081	6.520	5647	100.0	23.2	1.8	14.2	1.1	0.1	86	1.74
XC-94	499551	4692333	2092	Variscan basement	granite	25	7.716	657	30.231	2574	5.917	5426	99.7	24.9	1.3					2.04
XC-95	498000	4690449	1588	Variscan basement	granite	25	3.429	404	16.958	1998	6.776	5426	90.1	22.6	1.4					1.56

Table 2. (continued)

Sample Code	X	Y	Altitude, m	Tectonic Unit	Petrography	N	ρ_s	N_s	ρ_t	N_t	ρ_d	N_d	$P(\chi^2)$, %	Age, Ma	$\pm 1\sigma$, Ma	MTL, μm	SD, μm	SE, μm	N (L)	Dpar, μm
XC-96	505599	4660375	876	Variscan basement	granite	25	2.469	336	10.832	1474	7.090	5426	99.6	26.6	1.7	14.3	1.2	0.1	68	3.26
XC-98	505899	4664212	2254	Variscan basement	granite	25	1.666	143	8.052	691	6.679	5647	100.0	22.9	2.2	14.3	1.2	0.1	68	1.74
XC-100	504231	4682617	1110	Variscan basement	granite	25	2.410	179	10.164	755	6.458	5647	100.0	25.4	2.2	14.3	1.2	0.1	68	2.02
XC-102	491762	4669028	443	Variscan basement	granite	21	2.371	85	8.230	295	6.238	5647	100.0	29.8	3.8	13.9	1.2	0.1	71	1.93
XC-103	495552	4672943	1375	Variscan basement	granite	25	1.713	150	8.601	753	6.029	5647	100.0	19.9	1.9	13.9	1.2	0.1	71	1.51
XC-105	512804	4649935	1950	Variscan basement	granite	25	3.530	518	14.413	2115	7.717	5426	97.3	31.1	1.7	14.3	1.0	0.1	94	2.22
XC-106	508337	4668458	942	Variscan basement	granite	25	1.306	150	8.185	940	7.592	5426	97.7	19.9	1.8	14.3	1.0	0.1	94	1.69
XC-110	512219	4658479	1667	Variscan basement	granite	26	1.091	83	4.126	314	5.927	5647	100.0	26.0	3.3	14.3	1.0	0.1	94	1.69
XC-114	516200	4674762	322	Eocene flysch	conglomerate	50	9.171	988	33.872	3649	5.978	5647	91.9	26.8	1.2	14.3	1.0	0.1	94	1.64
XC-116	518436	4710083	1448	Tenda Massif	orthogneiss	35	1.471	175	9.565	1138	6.414	5647	100.0	16.4	1.4	14.3	1.0	0.1	94	2.33
XC-117	497567	4679152	2319	Variscan basement	granite	25	1.234	120	5.501	535	6.282	5647	100.0	23.4	2.4	14.3	1.0	0.1	94	1.99
XC-118	495026	4676143	2098	Variscan basement	granite	25	2.012	197	10.396	1018	7.278	5426	93.6	23.2	1.9	14.3	1.0	0.1	94	1.50
XC-122	511286	4655519	2273	Variscan basement	granite	25	3.648	455	11.672	1456	6.650	5426	100.0	34.2	2.0	14.3	1.0	0.1	94	2.55
XC-123x	510881	4631761	1702	Variscan basement	granite	26	1.601	222	7.125	988	7.027	5426	89.1	26.0	2.0	14.3	1.0	0.1	94	2.21
XC-125	493486	4668642	500	Variscan basement	granite	30	2.156	283	8.463	1111	6.713	5426	98.8	28.1	2.0	14.3	1.0	0.1	94	3.04
XC-132	527956	4649430	140	Eocene flysch	arkose	25	3.894	366	23.025	2164	5.978	5193	99.8	16.4	1.0	13.6	1.5	0.2	67	1.56
XC-133	532680	4634195	30	Eocene flysch	arkose	30	5.074	432	25.627	2182	6.208	5193	95.1	19.9	1.2	13.7	1.4	0.2	75	1.50
XC-134	533453	4624534	20	Eocene flysch	arkose	25	5.791	399	23.061	1589	5.519	5193	95.2	22.5	1.4	13.9	1.0	0.1	67	1.52
XC-135	527680	4614182	160	Variscan basement	granite	31	3.314	392	9.527	1127	6.323	5193	67.7	35.7	2.3	13.8	1.5	0.2	90	1.71
XC-136a	527847	4603189	72	Eocene flysch	arkose	30	6.518	721	25.558	2827	6.381	5193	96.7	26.4	1.3	14.0	1.3	0.1	101	3.07
XC-138	497023	4636935	580	Variscan basement	granite	25	3.773	368	13.953	1361	6.151	5193	93.0	27.0	1.7	13.9	1.1	0.1	50	1.71
XC-142	476954	4656929	20	Variscan basement	granite	30	2.050	236	7.826	901	6.093	5193	100.0	22.9	2.0	13.9	1.1	0.1	54	1.54
XC-143	466297	4664907	120	Variscan basement	granite	25	2.826	311	12.178	1340	6.036	5193	100.0	22.7	1.5	13.6	1.6	0.2	100	1.55
XC-144	482427	4667932	480	Variscan basement	granite	25	2.699	380	11.940	1681	5.634	5193	99.5	20.7	1.3	13.6	1.6	0.2	100	1.52
XC-148	506041	4714089	787	Eocene flysch	arkose	25	7.673	393	31.100	1593	5.691	5193	98.6	22.8	1.4	13.6	1.6	0.2	100	3.73
XC-149	504357	4714672	770	Eocene flysch	arkose	25	4.584	315	21.932	1507	6.266	5193	98.1	21.2	1.4	13.6	1.6	0.2	100	1.65
XC-151	479928	4702645	443	Variscan basement	granite	25	10.087	569	57.400	3238	5.749	5193	62.6	16.4	0.9	13.5	1.5	0.2	90	1.54
XC-152	489803	4683398	960	Variscan basement	granite	25	1.846	221	9.671	1158	6.763	5193	99.4	20.9	1.6	13.5	1.5	0.2	90	1.50
KU-22	515936	4593844	310	Variscan basement	granite	32	5.150	785	5.603	854	6.603	5193	89.6	97.9	5.4	13.8	1.2	0.2	65	3.76
KU-24	510880	4631740	1702	Variscan basement	granite	34	3.321	451	11.120	1510	5.864	5193	93.8	28.4	1.7	13.8	1.2	0.2	65	1.53

^aN is number of dated apatite crystals; ρ_s (ρ_t) are spontaneous (induced) track densities ($\times 10^5$ tracks/cm²); N_s (N_t) is number of counted spontaneous (induced) tracks; ρ_d is dosimeter track density ($\times 10^5$ tracks/cm²); N_d is number of tracks counted on dosimeter; $P(\chi^2)$ is probability of obtaining Chi-square value (χ^2) for n degree of freedom (where n is number of crystals minus 1); age $\pm 1\sigma$ is central age ± 1 standard error [Gauthier and Laslett, 1993]; MTL is mean track length; SE is standard error of mean track length; SD is standard deviation of track length distribution; N (L) is number of horizontal confined tracks measured; Dpar is average etch pit diameter of fission tracks. Ages were calculated using zeta calibration method [Hurford and Green, 1983], glass dosimeter CN-5, and zeta value of 324.93 ± 6.46 yr/cm².

[21] Track length distributions were measured in 29 samples (Table 2 and Figure 5). The mean confined track lengths (MTL) vary between $12.2 \pm 0.2 \mu\text{m}$ (XC-2) and $14.8 \pm 0.1 \mu\text{m}$ (XC-33) with standard deviations (SD) between 0.7 (XC-59) and $2.2 \mu\text{m}$ (XC-2). All samples, with one exception (XC-2), are unimodal and negatively skewed. These samples are characterized either by long MTL ($\geq 14 \mu\text{m}$) and short SD ($\leq 1 \mu\text{m}$), typical for rapidly cooled rocks with fast passage through the APAZ, or by slightly shorter MTL ($13.2\text{--}14 \mu\text{m}$) and larger SD ($1\text{--}1.6 \mu\text{m}$), pointing to a slower cooling through the APAZ. Sample XC-2 exhibits a broad (SD = $2.2 \mu\text{m}$), bimodal track length distribution with very short MTL ($12.2 \pm 0.2 \mu\text{m}$), attesting to a complex thermal history [Gleadow *et al.*, 1986a, 1986b].

[22] Dpar values range from 1.5 to $4.5 \mu\text{m}$ (Table 2), pointing to a variable chemical composition of the samples. In the majority of samples the Dpar values are small ($\leq 1.7 \mu\text{m}$), from which we infer a fluorine-apatite composition in these samples. There is no correlation between Dpar and age of the samples.

6. Interpretation and Discussion

6.1. Zircon FT Data

[23] Samples analyzed by ZFT analysis yield ages in the range $\sim 160\text{--}140$ Ma. These values are in line with the older data presented by *Carpéna et al.* [1979] and *Mailhé et al.* [1986]. Nevertheless, a full integration of the existing data sets is not possible, since the cited publications provide neither the analytical procedure nor the sample coordinates and the counting statistics. Yet there is valuable information that can be taken for further interpretation. According to clusters in the ZFT age pattern, we subdivide Corsica into three domains (referred to as ZFT domains, Figure 3a):

[24] Domain I encompasses the major part of Variscan Corsica with zircon ages in the range $244\text{--}147$ Ma (with one exception, 128 Ma). *Mailhé et al.* [1986] interpreted this age pattern as a west-to-east younging trend, resulting from westward decreasing thickness of Alpine thrust sheets that caused partial resetting of Variscan ZFT ages during thrusting. In fact, these authors considered the ZFT ages from Variscan Corsica as apparent ages, which means Variscan ages partially reset during Alpine metamorphism. In contrast, *Vance* [1999] recognized that ZFT ages in the range $220\text{--}100$ Ma are widely preserved within and adjacent to the western Alps orogenic system and interpreted them to be the result of high heat flow related to mantle upwelling during Late Triassic and Early Jurassic rifting and subsequent opening of the Ligurian-Penninic Ocean [Dunkl *et al.*, 1999]. This thermal event was long-lasting and characterized by extremely high heat flow on both continental margins [Vance, 1999]. We think that the ages evidently lack Tertiary rejuvenation. We therefore interpret these ages, following *Vance* [1999], as being related to the thermal event associated with the rifting and opening of the Ligurian-Piedmont Ocean. There are several evidences favoring such an origin of the ZFT ages: (1) the ZFT ages fit to the supposed time interval of mantle upwelling during

rifting and opening of the Ligurian-Piedmont Ocean; (2) the ages are getting older toward the west in their present position, away from the rifted continental margin and the heat source (details of this process are given by *Gallagher et al.* [1998]); (3) the ages are similar to “Ligurian-Piedmont” ZFT ages reported from different areas of the Alps; and (4) it is improbable that Tertiary Alpine metamorphism would have uniformly and systematically partially reset pre-Alpine (or Variscan) ZFT ages to Jurassic ages over wide areas, extending from Variscan Corsica to the Alps including the South Alpine realm, which experienced no Alpine metamorphism.

[25] The three Triassic ages (244 , 225 and 222 Ma) in the NW coast may deserve another explanation. They can be interpreted either as cooling ages recording Permian magmatic activity or post-Variscan erosion, or as originally Variscan ages that were partially reset by the thermal event related to the Jurassic rifting. We prefer the second option since the pattern of ages increasing with increasing distance away from the rift margin fits to the interpretation of “Ligurian-Piedmont”-related ZFT ages. So, this part of Variscan basement was too far from the heat source during the Jurassic rifting, therefore the temperature was too low to cause total resetting of the ZFT system.

[26] Domain II occupies a strip along the Alpine deformation front with Late Cretaceous to Paleocene ZFT ages (120 to 58 Ma, Figure 3a). Ages in this range were first presented by *Mailhé et al.* [1986] but were not considered by other authors (see section 3). However, a more recent study of *Zattin et al.* [2001] reported very similar ages probably from the identical region (neither the exact sample locations nor the relation to tectonic units are given by *Mailhé et al.* [1986] and *Zattin et al.* [2001]). Thus this age group seems to be geologically meaningful and can give an age constraint to the Alpine tectonic burial or perhaps postmetamorphic cooling of the Variscan basement.

[27] These ages neither conform with the Jurassic thermal event (ZFT domain I) nor with Alpine thrusting and denudation (ZFT domain III, see below). Although a Late Cretaceous age for HP/LT metamorphism is reported from the ophiolitic nappes [Lahondère and Guerrot, 1997], the European margin with its Variscan basement was not incorporated in the subduction/thrusting process before Eocene times, as it is shown by flysch cover (late Paleocene to middle Eocene).

[28] Therefore we interpret the ZFT ages of Domain II as apparent ages. Prior to collision, these ages were probably Jurassic and belonged to Domain I. In the Eocene, this part of the basement was buried by eastward subduction to a depth with temperatures sufficient for partial resetting of the ZFT ages. A conversion of temperature to depth, by assuming a thermal gradient of $10^\circ\text{C}/\text{km}$ reasonable for subduction zones [Turcotte and Schubert, 2002], revealed a burial depth of at least ~ 20 km, implying that a large part of ZFT domain I was substantially buried during collision, too.

[29] Domain III covers most of Alpine Corsica where ZFT ages are in the range of $45\text{--}19$ Ma (Figure 3a). These ages are in accord with $^{40}\text{Ar}/^{39}\text{Ar}$ ages on micas, ranging between 45 and 22 Ma [Brunet *et al.*, 2000], and indicate

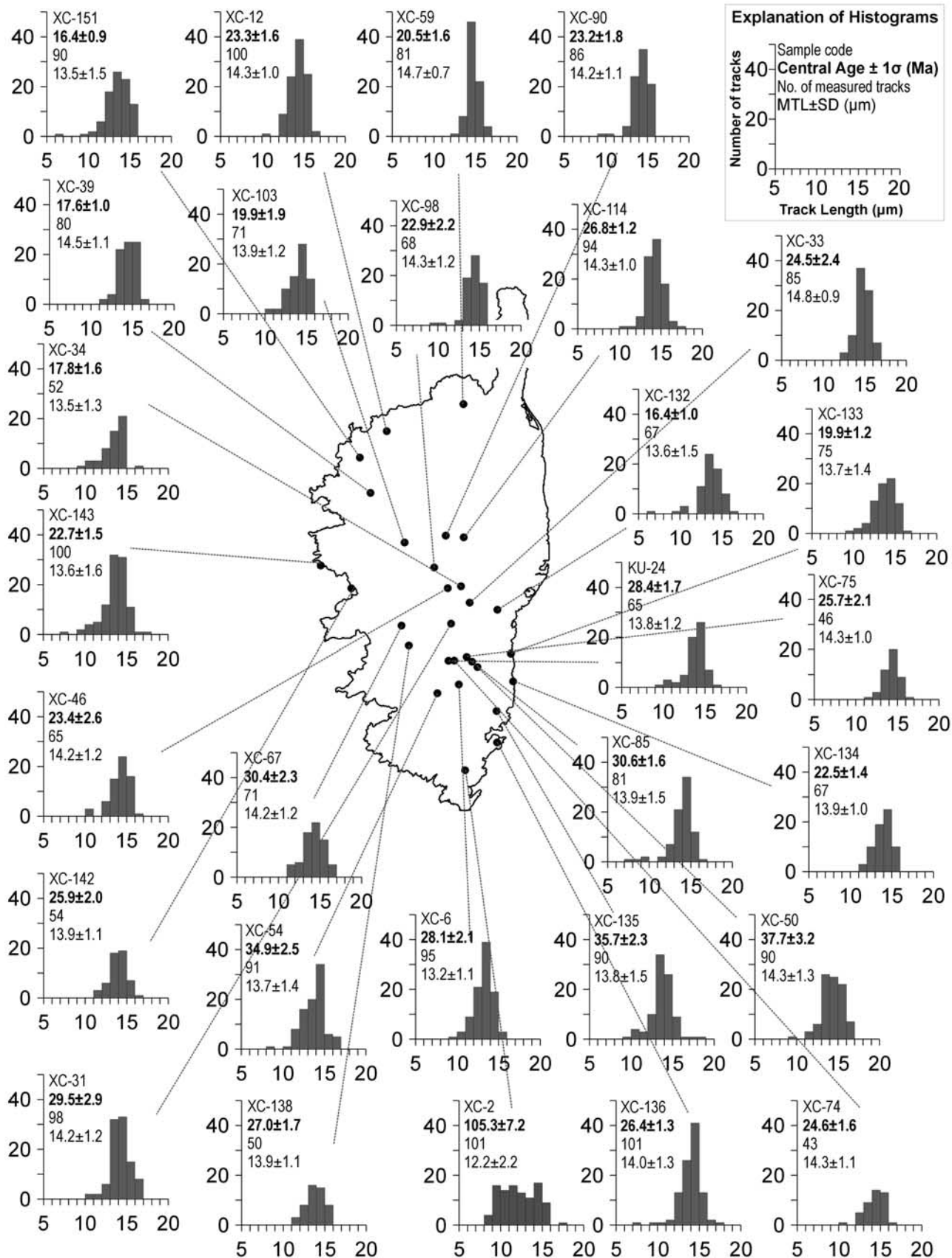


Figure 5. Confined track length distributions of apatites.

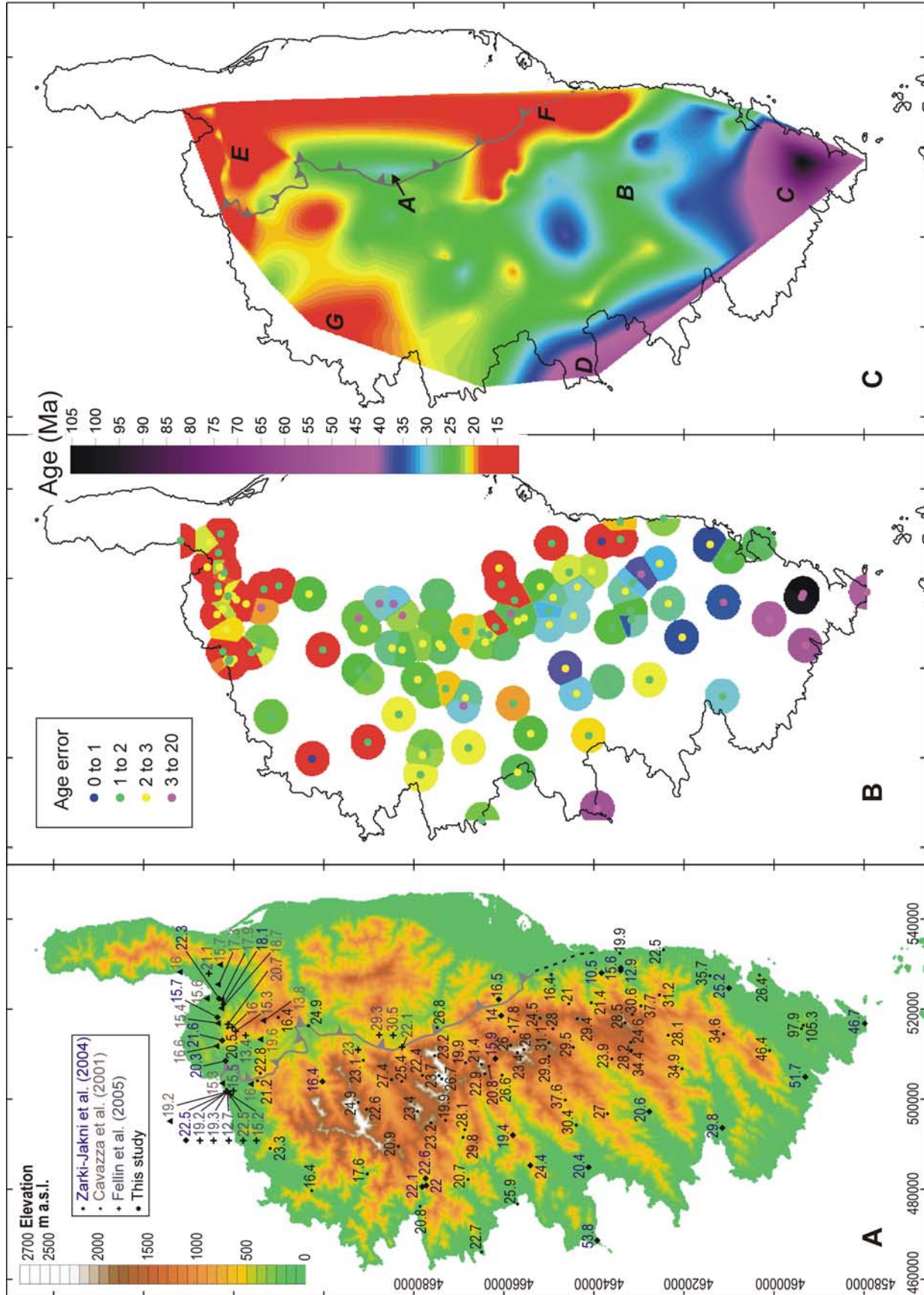


Figure 6

cooling following the thermal peak of early Tertiary metamorphism. In the early Oligocene, at ~ 33 Ma, the compressional regime changed to an extensional one [Jolivet *et al.*, 1990; Fournier *et al.*, 1991; Brunet *et al.*, 2000], the accretionary complex started to collapse, thrust planes were reactivated as normal faults, and the units were tectonically exhumed, partly as core complexes [Rosenbaum *et al.*, 2005]. According to $^{40}\text{Ar}/^{39}\text{Ar}$ and ZFT data, the time of the extensional regime can be bracketed between 33 and 19 Ma.

6.2. Apatite FT Data

6.2.1. Treatment Procedure on AFT Data Sets of Previous Studies

[30] As already advised in section 3, the data set of the previous studies requires some critical evaluation prior to integration. We filtered them according to the following criteria: (1) FT dating procedure must be reported; (2) localization of the samples must be given in some kind of coordinate system; (3) 15 or more apatite crystals must have been counted per sample in order to provide statistically robust results; and (4) when presenting track length distributions, at least 35 horizontal confined tracks must have been measured per sample, and standard deviation and standard error must have been reported.

[31] The data fulfilling these conditions were rectified to the UTM32/WGS84 coordinate system and used for further interpretation. Around 20 AFT ages and 1 track length distribution were excluded; the obtained database is presented in Figure 6.

6.2.2. Trends and Pattern in AFT Data

6.2.2.1. Age-Elevation Pattern and Exhumation Rates

[32] The age-elevation relationship of all samples shows no evident correlation: the data form one cluster with two outliers, the trend is not clearly positive or negative, but rather vertical [Danišík, 2005]. This feature is not surprising since it is known that Corsica does not form a single tectonic block, but is fragmented by a complex network of faults. The tectonic activity occurred after cooling of the basement through the APAZ. The island was segmented into numerous blocks, which experienced tilting and differential vertical and lateral displacement, and therefore the FT ages from foothills can be older than those from the mountain tops [Fellin *et al.*, 2005b].

[33] Nevertheless, we tried to calculate exhumation rates by the elevation-dependent method in individual profiles [Wagner and Reimer, 1972; Wagner *et al.*, 1977], which does not require knowledge of the geothermal gradient [Mancktelow and Grasemann, 1997]. We sampled seven elevation profiles in regions with steep relief in the central part of Variscan Corsica from single tectonic blocks sup-

posedly undisturbed by faults (Figure 7a). In all cases the samples yielded positive age-elevation relationships (Figure 7b). The maximum relief was less than 2000 m, topographic wavelengths in the range of 15–20 km (Figure 7c). The combination of these parameters rules out that topography disturbed the 110°C isotherm, as far as exhumation rates did not exceed 500 m/Myr [Stüwe *et al.*, 1994; Mancktelow and Grasemann, 1997; Stüwe and Hintermüller, 2000; Braun, 2002]. The exhumation rates were computed as error-weighted linear best fit by using a one-dimensional model and assuming the isotherm to be a horizontal plane. Finite exhumation rates are presented in Figure 7b and range between ~ 190 and 450 m/Myr. This indicates moderate cooling of the basement during late Oligocene to early Miocene times and a certain fluctuation in the exhumation rates between the sampled tectonic blocks.

6.2.2.2. Trends in Track Length Data

[34] In order to detect some trends in the AFT data, the AFT ages were plotted against MTL and SD. These relationships (Figure 8) show that most samples belong to a distinct cluster with AFT ages of ~ 10 to 40 Ma, relatively long MTL of $> \sim 13.3 \mu\text{m}$, and relatively narrow track length distributions expressed by low SD values ($< 2 \mu\text{m}$). These samples experienced cooling through the APAZ in a single, rapid process but not at the same time. Besides, there are few samples outside this cluster, with highly scattering ages (12 to 105 Ma), shorter MTL ($< 13.3 \mu\text{m}$), and broader track length distributions (SD $> 2 \mu\text{m}$). These samples did not experience a single-stage cooling history resided for a relatively long time within the APAZ or were reheated to the temperatures of the APAZ after a first period of cooling.

[35] On this point, it may be worthwhile to discuss the track length data reported by Fellin *et al.* [2005a] from the Balagne region in Corsica. Fellin *et al.* presented seven track length distributions (a minimum of 35 lengths measured) of the samples coming from regions with AFT ages mostly less than 30 Ma. At the first glance their data seem not to be in accord with those published by Cavazza *et al.* [2001] and Zarki-Jakni *et al.* [2004] from the very same localities, who presented MTL values of up to 1 μm longer than those of Fellin *et al.* [2005a] (see Figure 3b). However, the bimodal shape of some distributions in the Corte, Balagne and St. Florent regions presented by Fellin *et al.* [2005a] provide evidence that the cooling history of some localities is complex and can vary over distances of a few tens of meters and is controlled by the activity of faults [Fellin *et al.*, 2005a].

6.2.3. Spatial Distribution of AFT Ages

[36] As already discussed, extensive faulting and block movements influenced the relations between AFT age and sample elevation. Therefore, in a first approach, the AFT

Figure 6. Database containing all available AFT data, which passed prescribed quality criteria (see in section 6.2.1). (a) DEM with contour of Alpine front and AFT ages expressed in Ma. Errors are not shown. (b) AFT ages expressed as circles of 8 km diameter, where age values are indicated by the color of circles. error ranges (in Ma) are small dots in the center of the circles; values are indicated by colors. (c) Pattern of AFT ages obtained by interpolation and smoothing of the data set. Errors are not included; italic letters indicate clusters (see text for explanation), note that linking between areas E and F, and between C and D, is not based on the existing data but is an effect of interpolation.

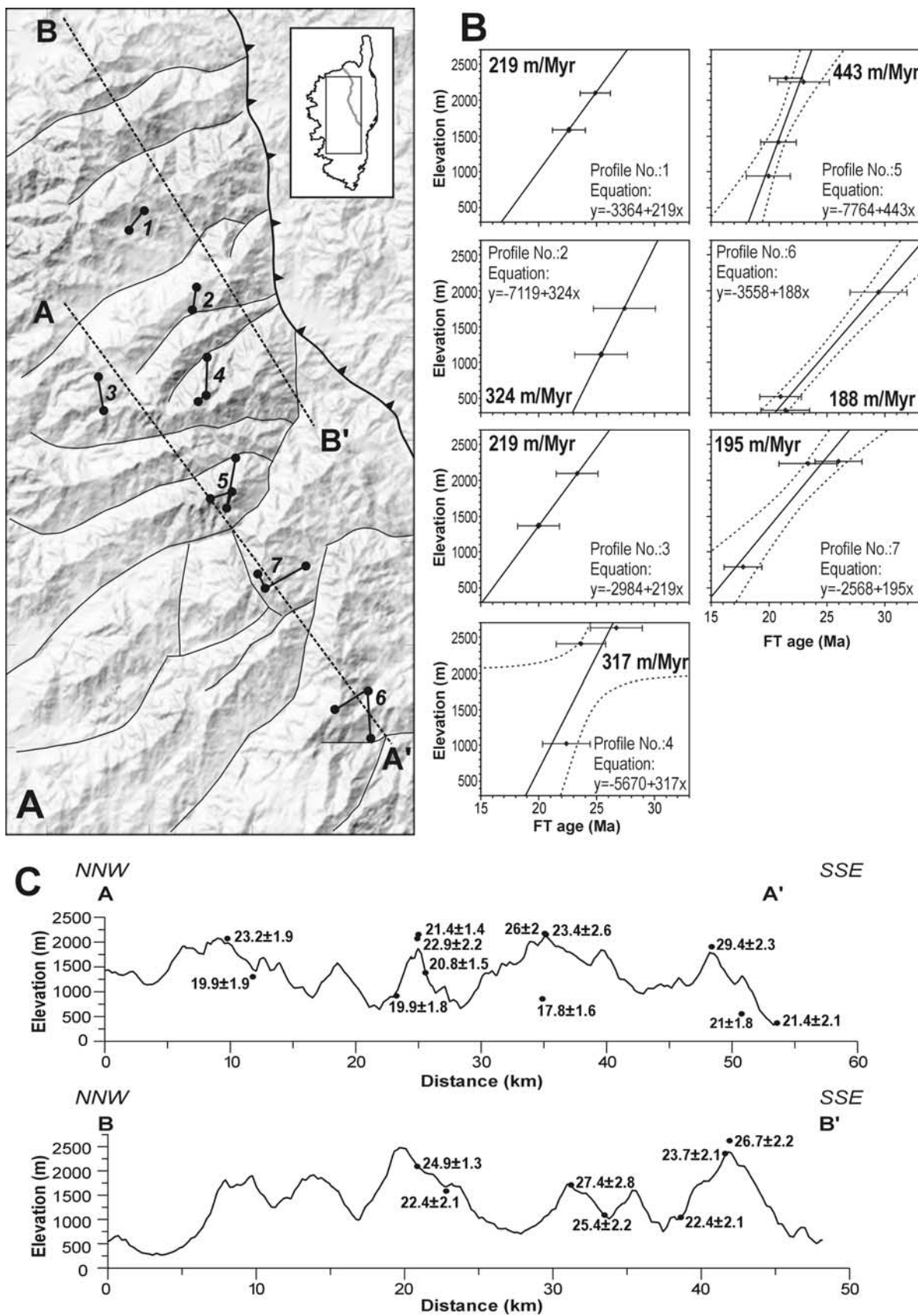


Figure 7

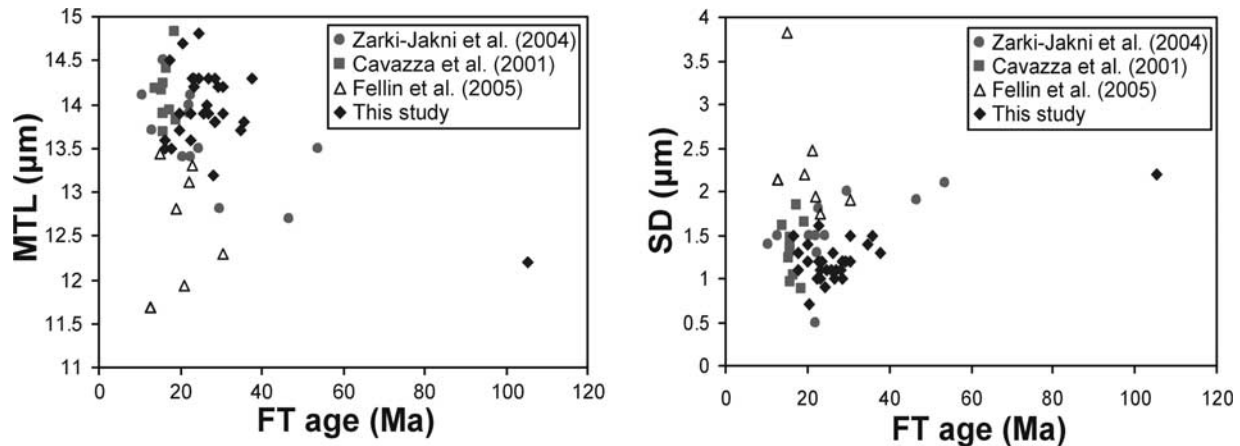


Figure 8. Relationships of AFT age, mean track length (MTL), and standard deviation (SD) of track length distributions.

ages can be evaluated in their spatial distribution without considering their elevation. In order to provide better visualization of the data set used for further work, the AFT ages are presented in three ways (Figures 6a, 6b, and 6c).

[37] The spatial distribution of AFT ages in Corsica reveals several patterns and trends. Most ages are reported from a W-E trending profile across the Tenda Massif and adjacent Alpine units in northern Corsica. Variscan Corsica is satisfactorily covered by the data in the central band running from SSE to NNW through the whole island, whereas the western peninsulas and the northwestern part call for more data. No AFT data are available from a major part of Alpine Corsica.

[38] The AFT ages form a fairly complex mosaic with clusters of different size. Prevailing ages are in the range 20–27 Ma, encountered mainly in the central and western parts of the island and covering the major part of the Variscan basement and also the western margin of Alpine Corsica in its central part. The only exception in this cluster are two slightly higher ages of 30.5 ± 3.2 and 29.3 ± 3.6 Ma reported by *Fellin et al.* [2005a] from the Corte region close to the Alpine front (denoted with “A” in Figure 6c).

[39] Further to the south, a cluster of slightly higher ages in the range of 35–25 Ma can be identified (“B” in Figure 6c). The southernmost extremity of Corsica is characterized by the highest AFT ages around 50 Ma, with two exceptionally high ages of 105.3 ± 7.2 and 97.9 ± 5.4 Ma (“C” in Figure 6c). An age of 53.8 ± 4.1 Ma was reported by *Zarki-Jakni et al.* [2004] from the westernmost extremity of a peninsula west of Ajaccio (“D” in Figure 6c).

[40] The youngest ages in the range of 10–23 Ma form two well-defined and one ill-defined clusters. One well-defined cluster is located in the northern part of Corsica and covers the Tenda Massif and Alpine nappes around the St. Florent

region (“E” in Figure 6c). The second cluster covers the area along the southern part of the Alpine front, southwest of the Oriental Plain (“F” in Figure 6c). The remaining ill-defined cluster (23–15 Ma) can be identified in the northwestern part of Variscan Corsica (“G” in Figure 6c). This cluster may in fact belong to the young age group of the Tenda region, but there is a gap in data in between.

6.2.4. Subdivision Into AFT Domains

[41] In order to interpret the complex pattern of the AFT data, we divided Corsica into four AFT domains.

[42] AFT domain I comprises all occurrences of Eocene flysch along the border zone between Alpine and Variscan Corsica (Figure 9a). AFT ages range from 30.6 ± 1.6 (XC-85) to 16.4 ± 1 Ma (XC-132) and are all younger than the depositional age, indicating thermal resetting after deposition. In addition, all track length distributions are unimodal, negatively skewed, with MTL from 13.6 ± 0.2 (XC-132) to 14.3 ± 0.1 μm (XC-114) and SD from 1 (XC-114) to 1.5 μm (XC-132), which is indicative of moderate to fast cooling through the APAZ. Thermal history modeling was constrained by the depositional age of the sediments (~56–40 Ma, early to middle Eocene [*Durand-Delga, 1978; Rossi et al., 1980*]) and revealed fairly similar cooling paths for all samples (Figures 10a and 10b): After deposition the samples were heated to temperatures $>120^\circ\text{C}$ and the tracks completely annealed. Resetting was followed by fast cooling to near-surface conditions, where the samples stayed until present.

[43] The tT path is interpreted as follows: during the Eocene collision, the flysch was deposited in the trough in front of the approaching Alpine nappes. As the collision continued, flysch was progressively buried below an increasing rock column until the AFT memory was reset at temperatures above 120°C . Two questions arise in this

Figure 7. (a) Shaded DEM showing sample localities of elevation profiles (labeled with numbers), which represent individual blocks. (b) Age-elevation plots of profiles (profile numbers as in Figure 7a). Exhumation rates (in m/Myr) are calculated as error-weighted linear best fit (solid line) with 95% confidence level (dashed lines). (c) Topographic profiles (for location, see Figure 7a) showing AFT ages. See text for explanation.

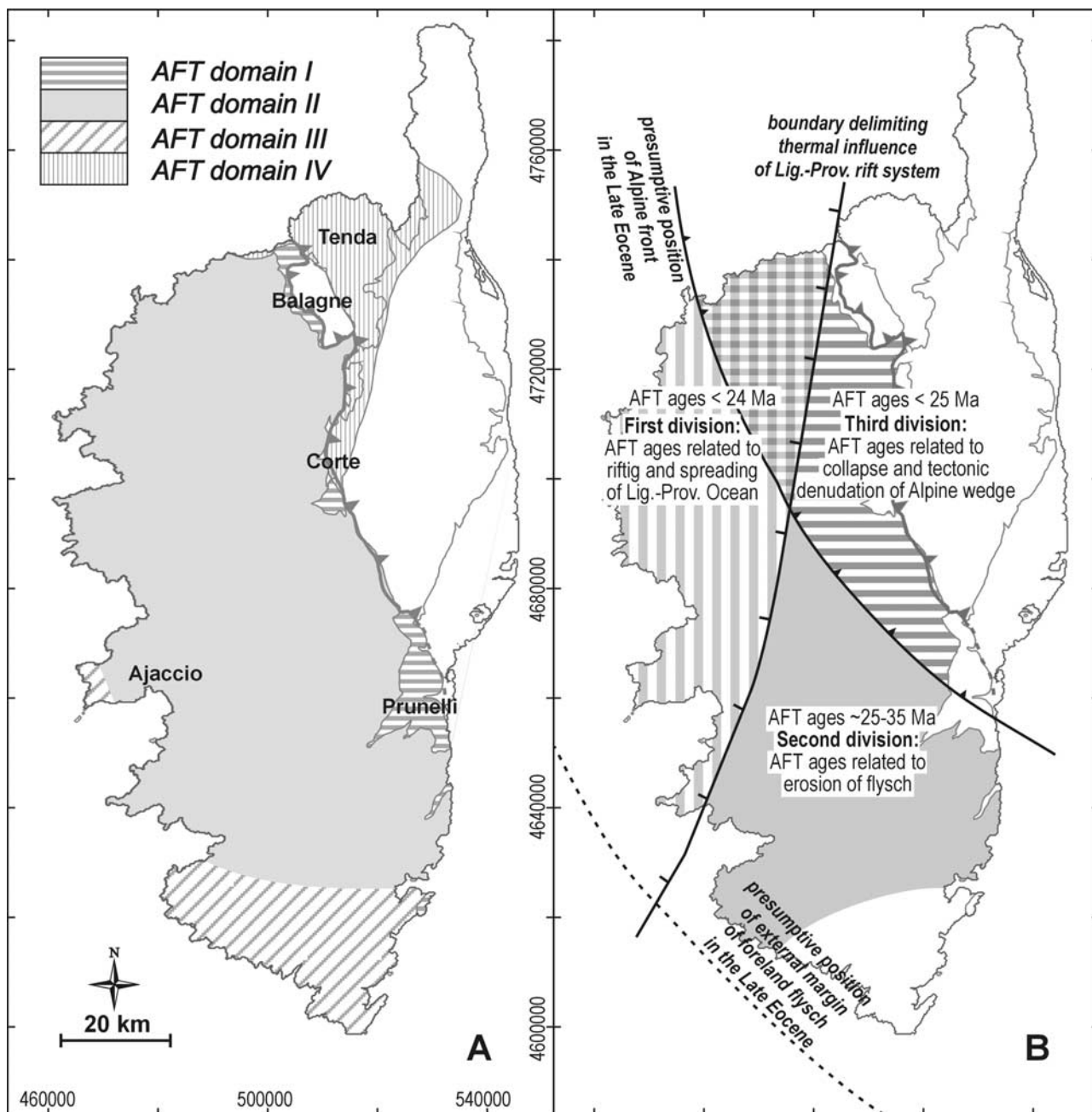


Figure 9. (a) Subdivision of Corsica into AFT domains. See text for explanation. (b) Illustration showing a subdivision of AFT domain II into three subdivisions according to similarities in AFT ages and relations to geological features (as reconstructed in section 6.2.4, see text for explanation).

point: (1) Of what type was the cover under which the samples were buried? (2) What was the thickness of the cover?

[44] The first question to be addressed involves the composition of the cover. The relation of the Eocene flysch to the Variscan and Alpine units is complex and changes from north to south [Egal, 1992]. In the northern and central areas of Corsica, in the Balagne and Corte regions, Eocene flysch formations are essentially autochthonous with regard to the Variscan basement, but are largely overlain by Alpine

nappes. *Bézert and Caby* [1988, 1989] described blue amphibole in the Bartonian flysch near Corte, indicating metamorphic conditions of $P = 0.5 \text{ GPa}$ and $T = 300 \pm 50^\circ\text{C}$. This means that the flysch in northern and central Corsica was involved in the subduction process.

[45] Further to the south, in the Prunelli region, the flysch is largely undeformed, devoid of metamorphic assemblages and shows onlap on the Variscan basement and the Alpine nappes [Egal, 1992]. The Prunelli flysch was not involved in the subduction process but represents a distal part, which

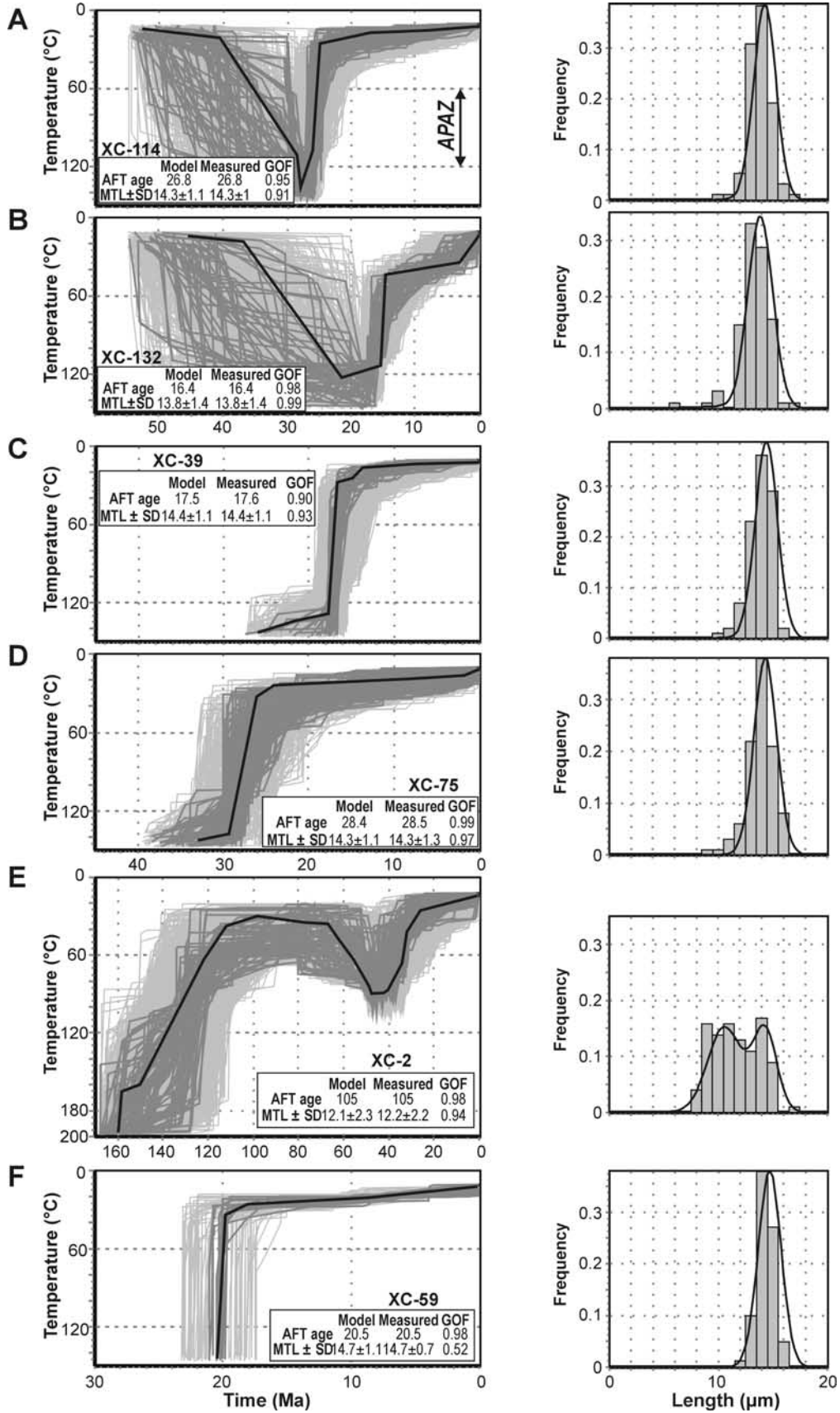


Figure 10

remained outside the accretionary wedge. Nevertheless, AFT ages show resetting and imply burial below a thick rock column. If the observations of *Egal* [1992] are correct, the resetting of the AFT ages in the Prunelli flysch must have been induced by a thick flysch sequence without tectonic thickening. Estimation of the thickness of the covering rock column can be deduced from the thermal modeling results, but is critically dependent on the thermal gradient. Present-day geothermal gradients for Corsica are moderate and range from 26 to 31°C/km [*Lucazeau and Mailhé*, 1986]. It is likely that during the Tertiary the geothermal gradient was fluctuating, decreased during collision and increased during rifting. When suggesting high values of 35–40°C/km during rifting (thus constraining minimum burial thickness), a thickness of the cover that loaded the actually exposed flysch samples was at least 2.5 km. This suggests that during Eocene collision probably all of Variscan Corsica was covered by a pile of foreland flysch. This pile was later significantly eroded so that only small remnants are preserved. This idea is elaborated below.

[46] AFT domain II encompasses the majority of the Variscan basement except its southernmost part and the peninsula west of Ajaccio (Figure 9a). The AFT ages in this domain exhibit a fairly wide range between 34.6 ± 3.3 and 16.4 ± 0.9 Ma, suggesting cooling during Oligocene and Miocene times. Track length distributions are unimodal, narrow ($SD \leq 1 \mu\text{m}$), with long MTL ($\geq 13.8 \mu\text{m}$), and point to fast cooling. Thermal history modeling reveals similar tT paths for all modeled samples, characterized by fast cooling through the APAZ followed by a period of modest decrease in temperature until present (Figures 10c and 10d). Fast cooling, however, occurred in different periods: samples from the south cooled through the APAZ in the Oligocene, whereas samples toward the NNW experienced cooling in Miocene times. This time interval delimited by AFT data was a period of “tectonic reorganization”, which completely changed the picture of the western Mediterranean region. The events important for the interpretation of the AFT data can be reviewed as follows: (1) Alpine collision with top-to-west sense of shear lasted until ~ 33 Ma and created an accretionary wedge partly covering Variscan Corsica [*Brunet et al.*, 2000]; (2) at ~ 33 Ma, the boundary conditions changed from compression to extension and the overthickened crust started to collapse, which led to exhumation of buried units [*Jolivet et al.*, 1990, 1998; *Brunet et al.*, 2000]; (3) from ~ 33 to 25 Ma, the Alpine thrust front was reactivated as ductile to brittle-ductile shear zones with top-to-east sense of shear, as recorded by $^{40}\text{Ar}/^{39}\text{Ar}$ data [*Jolivet et al.*, 1990; *Fournier et al.*, 1991; *Brunet et al.*,

2000]; (4) at ~ 30 Ma rifting of the Ligurian-Provençal Basin started. This event is recorded by synrift sediments in the Gulf of Lion (29 Ma [see *Gorini et al.*, 1993; *Chamot-Rooke et al.*, 1999; *Sérrane*, 1999]), on the Sardinian margin (30 Ma, *Cherchi and Montadert* [1982]), and in SW Corsica (25 Ma [*Ferrandini et al.*, 1999]); and (5) the following drifting event is constrained by the counterclockwise rotation of the Corsica-Sardinia block between 21 and 16 Ma [*Vigliotti and Kent*, 1990; *Van der Voo*, 1993; *Chamot-Rooke et al.*, 1999].

[47] The denudation of AFT domain II can be linked either to the rifting before the formation of the Ligurian-Provençal Basin or to the collapse of the wedge, or to both of them. This relationship can be examined by plotting the AFT ages as a function of distance to representative markers. When the ages are only related to the Ligurian-Provençal rift system, they should become younger in westward direction toward the rift margin, and the ages closest to the margin should be of the same age or younger than the start of ocean spreading [*Gallagher and Brown*, 1997; *Gallagher et al.*, 1998]. In contrast, when the ages are related to the collapse of the wedge, they should become younger in eastward direction toward the wedge front. In case that the ages are related to both, rifting and wedge collapse, a sort of “antagonistic” trends can be expected: the ages should increase from west to east and concurrently from east to west.

[48] To test this hypothesis, the AFT ages of AFT domain II were plotted (1) as a function of distance between sampling points and a boundary of the transitional domain of the Ligurian-Provençal rift and continental margin as defined by *Rollet et al.* [2002], and (2) as a function of distance between sampling points and present-day Alpine front (Figure 11). In both cases there are ill-defined trends reflecting a decrease in age toward the defined boundaries. This indicates that cooling and denudation of the basement could indeed be related to both the Ligurian-Provençal rift system and to the collapse of the Alpine wedge. Both processes were contemporaneous during Oligocene tectonic reorganization and did overlap in space. Their interplay governed the exhumation of the basement.

[49] It might be speculated to attribute specific ages of AFT domain II to one of these two processes. This could be realized when we sketch the assumed maximum extent of the orogenic wedge and the external boundary of the zone thermally affected by rifting. The first one is reconstructed in section 7 (see below). The latter one can be reconstructed from the present-day position of the rift, and from the assumption that AFT ages are younger or of the same age

Figure 10. Thermal modeling results of AFT data of representative samples from AFT domains (a,b) I, (c, d) II, (e) III, and (f) IV obtained with HeFTy program [*Ketcham*, 2005]. Results are displayed in time-temperature diagrams (left diagrams). Light gray paths indicate acceptable fit; dark gray paths indicate good fit; thick black line indicates best fit; MTL is mean track length in μm ; SD is standard deviation in μm ; GOF is goodness of fit (statistical comparison of the measured input data and modeled output data, where a “good” result corresponds to value 0.5 or higher, “the best” result corresponds to value 1). Frequency distribution of measured confined track length data (right diagrams) is overlain by a calculated probability density function (best fit). Note that modeled tT paths are valid only inside the APAZ; however, outside this temperature range they need not necessarily represent the real thermal trajectory of a sample.

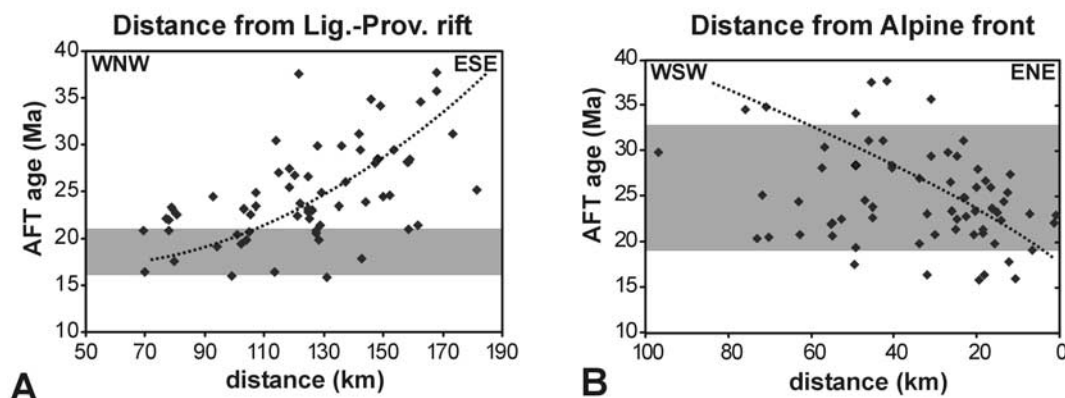


Figure 11. (a) AFT age as a function of distance from the Ligurian-Provençal rift. A trend of increasing ages away from the rift is visible. Grey band depicts the time of oceanic spreading. (b) AFT ages as a function of distance from the Alpine front, where an ill-defined trend of ages decreasing toward the front is visible. Grey band depicts the time of tectonic denudation as constrained by ZFT and $^{40}\text{Ar}/^{39}\text{Ar}$ data (see section 6.1).

as the onset of ocean spreading [Gallagher and Brown, 1997; Gallagher et al., 1998]. In this way the AFT domain II can be subdivided into three divisions (Figure 9b):

[50] The first division encompasses the NW part of Variscan basement with the ages younger than ~ 24 Ma, when the rifting in Corsica began. Ages within this division are interpreted as to be reset due to increased heat flow related to mantle upwelling during rifting and spreading of the Ligurian-Provençal Ocean.

[51] The second division covers the southern part, which was formerly covered by foreland sediments (see section 7). AFT ages (between ~ 25 and 35 Ma) indicate exhumation during the Oligocene. The exhumation, which led to the erosion of the flysch, was probably a consequence of isostatic rebound responding to the slab break-off in the east dipping Alpine subduction zone [Davies and von Blanckenburg, 1995; Malavieille et al., 1998]. Thus the denudation can be understood as erosional in origin.

[52] The third division encompasses the parts formerly involved in the subduction process. The AFT ages are younger than those of second division and range between ~ 25 and 15 Ma. They are younging toward the present-day Alpine front. In the Oligocene, the samples were exhumed from depths greater than those covered only by the flysch. Therefore they passed the APAZ in the early Miocene with a certain delay to division II. Denudation of this part of basement from below the Alpine nappes was largely of tectonic origin.

[53] First and third division overlap in the northern central part of Corsica (Figure 9b).

[54] AFT domain III encompasses the southernmost part of Variscan Corsica and the western extremity of the peninsula west of Ajaccio (Figure 9a). Samples from this domain yielded by far the oldest AFT ages (105.3 ± 7.2 to 46.4 ± 4 Ma) and bimodal track length distributions ($SD = 2.2 \mu\text{m}$) with by far the shortest MTL ($12.2 \pm 0.2 \mu\text{m}$). This points to a complex thermal history markedly different from those of the rest of the island. The Cretaceous apparent AFT

ages (105.3 ± 7.2 and 97.9 ± 5.4 Ma) are recognized for the first time in Corsica. They are the only samples from which a Mesozoic AFT memory of the crystalline basement is preserved. Thermal history modeling, constrained by the ZFT age of 159.8 ± 12.1 Ma (KU-22), reveals a tT path with cooling through the APAZ from the Middle Jurassic to the Early Cretaceous, stagnation above the APAZ until the Paleocene, then a temperature increase into the APAZ in the Eocene, and fast cooling to surface temperature in the Oligocene (Figure 10e). The modeled cooling path is interpreted as follows: after the Jurassic thermal event related to the opening of the Ligurian-Piedmont Ocean that is recorded by ZFT data (see section 6.1), the basement cooled through the APAZ at moderate rates. This cooling phase lasted until the middle Early Cretaceous.

[55] During mid-Cretaceous to Paleocene times, the actual exposed level of the basement resided in levels above the APAZ. The basement was probably exposed to erosion as can be inferred from the abundant occurrences of coarse grained detrital material derived from the Variscan basement in Cretaceous sequences preserved in the Alpine nappes [Rossi et al., 1980].

[56] In the Paleocene to Eocene, the modeling results reveal reheating to the levels of the APAZ. This period of heating goes conform with subduction and nappe stacking and indicates that this part of the basement was also buried beneath an increasing rock pile, although there is no direct evidence of the former presence of flysch or Alpine nappes in this region. The thickness of the cover estimated from the modeling results may have been in the order of 4–8 km, assuming a surface temperature of 10°C , a thermal gradient of 20 to $10^\circ\text{C}/\text{km}$, typical of thrust complexes, and a burial temperature ~ 70 – 90°C .

[57] The late Eocene to early Oligocene period is characterized by fast cooling to near-surface conditions followed by very slow cooling up to present. This fast cooling phase is the same like in AFT domain II and is interpreted as reflecting rapid erosion of the flysch.

[58] The NE part of Corsica, including the Tenda Massif, the St. Florent Basin, and adjacent regions make up the AFT domain IV (Figure 9a). The vast majority of the AFT data from this domain was reported by previous studies [Jakni *et al.*, 2000; Cavazza *et al.*, 2001; Fellin, 2003; Zarki-Jakni *et al.*, 2004; Fellin *et al.*, 2005a]. Additionally, we measured three AFT ages and one track length distribution on the samples from the Tenda Massif. Ages range from 24.9 ± 2.7 to 16.4 ± 1.4 Ma and indicate Miocene cooling. The track length distribution of sample XC-59 is unimodal, narrow ($SD = 0.7 \mu\text{m}$), with very long MTL ($14.7 \pm 0.1 \mu\text{m}$), and indicates fast cooling through the APAZ, in line with previous data. The modeled cooling path reveals fast cooling for the Tenda Massif (Figure 10f). An extremely high cooling rate (up to $60^\circ\text{C}/\text{Myr}$ that is equivalent to an exhumation rate of $\sim 2 \text{ km}/\text{Myr}$, assuming a thermal gradient of $30^\circ\text{C}/\text{km}$) is interpreted to reflect tectonic denudation of the Tenda Massif as a metamorphic core complex [Jolivet *et al.*, 1990; Fournier *et al.*, 1991; Rosenbaum *et al.*, 2005].

[59] A different thermal history was determined by Fellin *et al.* [2005a] in the St. Florent, Balagne, and Francardo regions, which surround the Tenda Massif and at present form morphological depressions (Balagne) or host Miocene basins (Francardo and St. Florent). These authors argued that the thermal history of the depressions (basins) is complex and controlled by the activity of minor faults. The cooling trajectories were perturbed by a heating event (from ~ 19 to 14 Ma), which is interpreted as being related to burial in the depressions during the deposition of up to $\sim 2 \text{ km}$ thick Miocene successions.

7. Tectonothermal Reconstruction and Comprehensive Model

[60] From the constraints presented above we attempt to reconstruct the former extent of the accretionary wedge and the foreland basin. The relevant constraints are (1) present-day Alpine Corsica, representing a reminder of the former wedge, encroaches the NE third of the island, and the Alpine front runs in a NNW-SSE direction; (2) part of the Variscan basement, above defined as ZFT domain II, reached the ZPAZ during Eocene, whereas ZFT domain I reached only temperature levels between APAZ and ZPAZ; (3) flysch from the Prunelli region is largely undeformed, in a normal stratigraphic position, and devoid of metamorphism. AFT ages are all reset implying burial of at least 2.5 km; (4) flysch from the Corte and Balagne regions is deformed, and became part of the subduction complex. It contains metamorphic assemblages indicating temperatures around 300°C , and the AFT ages are reset (see section 6.2.4); and (5) AFT domain IV was buried beneath an at least 4 km thick rock pile (see section 6.2.4).

[61] The restored sedimentary wedge of flysch is presented in Figure 12. Its front was running in a NNW-SSE direction in present coordinates and NNE-SSW in synsedimentary coordinates, and its thickness diminished away from the Alpine front. The flysch probably covered the entire Variscan basement of Corsica and filled an asymmetric foreland basin. The source area of granitic detritus for

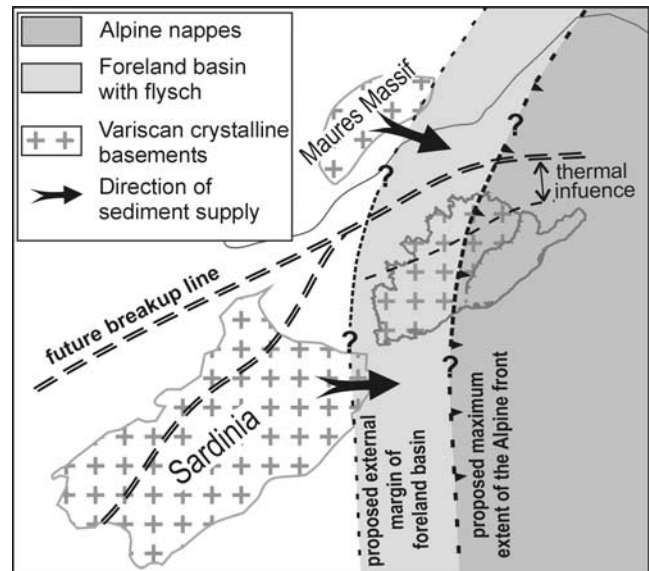


Figure 12. Suggested westward extent of Alpine nappe stack and foreland basin during Eocene collision at circa 40 Ma. Corsica-Sardinia block formed SE margin of European continent. Note that the tectonic boundaries north and south of Corsica are only approximate.

the flysch trough was therefore not the basement of Corsica itself as proposed in the literature [e.g., Durand-Delga, 1978] but rather adjacent regions like Sardinia or the Maures Massif, which were covered neither by the Alpine wedge nor by the foreland sediments at that time.

[62] We present a comprehensive model that consists of several time sections.

[63] In the Middle to Late Jurassic (~ 170 – 145 Ma), the Ligurian-Piedmont Ocean opened between the Gondwanan and Laurasian plates (the latter including Corsican crystalline basement [see Frisch, 1979, Figure 2]). Rifting and ocean opening was associated with increased heat flow related to mantle upwelling. The Variscan basement of Corsica was situated in the vicinity of the rift, as recorded by reset ZFT data. The first rocks of future Alpine Corsica were formed (ophiolites and deep-sea sediments) in the Ligurian-Piedmont Ocean.

[64] In the Early to early Late Cretaceous (~ 145 – 80 Ma), spreading of the Ligurian-Piedmont Ocean continued. The Variscan basement progressively cooled down, as indicated by AFT data in southern Corsica. The cooling is the consequence of retreat of the basement from the heat source (or spreading center) in the course of continuous ocean spreading.

[65] In the Late Cretaceous (probably around 80 Ma), an eastward dipping (in present coordinates) intraoceanic subduction zone developed in the Ligurian-Piedmont Ocean, which later led to the closure of this ocean and to collision between the European and Adriatic continents in early Tertiary times. In this time, a tectonically calm period characterized Variscan Corsica. The basement resided near surface conditions and was exposed to erosion as indicated

by occurrences of crystalline pebbles in some of the Alpine nappes. The sedimentary sequences of the Alpine nappes ended up with the Upper Cretaceous flysch, indicating tectonic activity. Subduction evidence is given by metamorphism of tectonic units of both oceanic and continental origin at HP/LT conditions. A Sm/Nd age of 83.8 ± 4.9 Ma [Lahondère and Guerrot, 1997] and a $^{40}\text{Ar}/^{39}\text{Ar}$ age of ~ 65 Ma [Brunet et al., 2000] testify that subduction already operated during Late Cretaceous time.

[66] In the Paleocene (~ 65 – 56 Ma), Variscan Corsica approached the subduction zone, and finally in the late Paleocene the first sediments of the foreland flysch trough were deposited on the basement, indicating the commencement of the Alpine collision and beginning of basement burial.

[67] The Eocene (~ 56 – 35 Ma) is characterized by the collision between Variscan and Alpine Corsica.

[68] According to the FT data, the entire Variscan basement was affected by the thermal effect of collision: either buried below flysch or overridden by Alpine nappes. Some of its easternmost marginal parts (Tenda Massif and Corte slices) were dragged down into the subduction zone and metamorphosed at HP/LT (blueschist facies) and then MP/LT (greenschist facies) conditions between ~ 45 and 32 Ma. The major part of the Variscan basement was residing at temperature levels between APAZ and ZPAZ, or within ZPAZ as indicated by partially reset ZFT ages. An exception was the southernmost part, where the AFT system was only partially reset at temperatures below $\sim 110^\circ\text{C}$. In the late Eocene, the final closure of the Ligurian-Piedmont oceanic basin resulted in the emplacement of ophiolitic nappes on parts of the foreland flysch.

[69] The Oligocene (~ 35 – 23 Ma) can be characterized as a period of tectonic reorganization, in which several tectonic events occurred contemporaneously. Until ~ 33 Ma a thick accretionary complex was built. Around 33 Ma the boundary conditions changed from compression to extension and the overthickened crust started to collapse and exhume. This stage of postorogenic extension was the consequence of isostatic rebound responding to the slab break-off in the east dipping Alpine subduction zone, and of eastward rollback of the newly formed Apennine subduction zone. First occurrences of synrift sediments in the Gulf of Lions indicate the inception of Ligurian-Provençal rifting between the future Corsica-Sardinia microplate and the European mainland.

[70] Variscan Corsica started to exhume by the removal of the thick cover from the top of the basement by erosional denudation in the major part of Variscan Corsica and by tectonic denudation in NE part of the island. The NW part of the basement was thermally affected by heating in the early Miocene related to the opening of the Ligurian-Provençal Basin. In Alpine Corsica, the Alpine thrust planes with top-to-west sense of shear were reactivated as ductile to ductile-brittle normal shear zones with top-to-east sense of shear, leading to exhumation of HP and MP metamorphic rocks along extensional detachments.

[71] In the Miocene (~ 24 – 5 Ma), extension still continued due to the eastward retreating Apennine subduction

zone. Consequently, at ~ 18 Ma rifting of the Tyrrhenian Basin started east of Corsica. Between ~ 21 and 16 Ma the Corsica-Sardinia block rotated counterclockwise close to its present position, and oceanic crust formed in the Ligurian-Provençal Basin. During rotation, Variscan Corsica was cut by subvertical faults, which defined block boundaries and later orientation of valleys. Exhumation continued, removing the cover from top of the basement. Corsica was uplifted to higher levels than the conjugated rift shoulder in the NW (Maures Massif), owing to an eastward shift of depleted asthenosphere with lower density beneath the Corsica-Sardinia block [Doglioni et al., 1999, 2004]. At ~ 17 Ma, Variscan Corsica provided material to sediment basins in the east. Individual blocks show differential exhumation.

Appendix A

A1. Fission Track Methodology

[72] Apatite and zircon crystals were recovered from whole rock samples using standard magnetic and heavy liquid separation techniques. Apatites were embedded in epoxy, zircons in PFA Teflon™. Prepared mounts with grains were polished to 4π geometry. Spontaneous tracks in apatites were revealed by etching with 5.5 M HNO_3 solution for 20 seconds at 21°C [Donelick et al., 1999]. Zircons were etched in an eutectic mixture of KOH and NaOH at 215°C for 20 to 80 hours [Zaun and Wagner, 1985].

[73] Uranium contents of the samples were assessed by irradiating with thermal neutrons, which induce fission in a proportion of ^{235}U sample atoms. The induced tracks were recorded in an external detector of low-uranium muscovite sheets (Goodfellow mica™), attached to the sample during irradiation [Gleadow, 1981]. Samples were irradiated in the thermal column of the TRIGA nuclear reactor at Oregon State University, Oregon, where Cd ratio is ~ 14 that is well suited to FT use. In the thermal facility, the reference value of neutron flux at the face (fully inserted) is 8×10^{10} n/cm² × sec; the flux gradient is approximately 2% per cm. Neutron fluence was monitored using the Corning glass dosimeters CN-2 (for zircons) and CN-5 (for apatites), with a known uranium content of 37 ppm and 12 ppm, respectively [Hurford and Green, 1982]. Requested neutron flux for apatite samples was 4.5×10^{15} n/cm² and 1.5×10^{15} n/cm² for zircon samples. The apatite and zircon samples were irradiated for ~ 16 and ~ 5 hours, respectively.

[74] After irradiation, mica detectors were etched in 40% HF for 30 minutes at 21°C . Finally, the mounts with corresponding micas were attached side by side on a glass slide. Spontaneous ^{238}U and induced ^{235}U fission tracks were counted under a Zeiss Axioskop 2, equipped with a digitizing tablet, red LED cursor, drawing tube attachment, and controlled by the computer program FT Stage version 3.11 [Dumitru, 1993]. Tracks in apatites and micadectors were counted with $1250\times$ magnification using dry objective, tracks in zircons were counted under same condition but using oil objective (Cargille oil type B, $n = 1.515$). Only crystals with well-polished surface parallel to the crystallographic c axis and homogenous uranium distribution were

analyzed, regardless of track density. The minimum of 21 grains from each sample was counted depending on the quality of mount. Lengths of horizontal confined tracks and Dpars in apatites were measured only on grains oriented parallel to the crystallographic c axis. A minimum of 43 horizontal confined tracks was measured in the samples in order to obtain representative and statistically robust distribution.

[75] The IUGS-recommended zeta calibration approach was used to determine the ages [Hurford and Green, 1983]. The zeta value of 324.93 ± 6.46 for dosimeter glass CN-5 and 123.92 ± 2.53 for dosimeter glass CN-2 has been derived by analyst M. Danišík from 13 determinations of apatites and 5 of zircons from the Fish Canyon Tuff, Durango apatite, and Tardree Rhyolite [Hurford, 1998]. FT ages were calculated with program TRACKKEY version 4.1 [Dunkl, 2002]. A detailed description of the analytical procedure used is given by Danišík [2005].

A2. Thermal History Modeling Based on AFT Data

[76] Thermal histories of the samples were modeled by the HeFTy Beta version 4 modeling program [Ketchum, 2005]. An inverse Monte Carlo algorithm with multikinetic annealing model [Ketchum et al., 1999] was used to generate tT paths. The algorithm generates a large number of tT paths, which are tested with respect to input data. The fitting of the measured input data and modeled output data is statistically evaluated and characterized by value of the goodness of fit (GOF). A “good” result corresponds to value 0.5 or higher, “the best” result corresponds to value 1 for both indicators. Results are presented in form of tT paths, passing statistical criteria and conforming to user-

entered constraints, that best reproduces the measured data. It has to be kept in mind that even a perfectly fitting and statistically proved model of thermal history must not necessarily correspond to the real history of a sample. To avoid misinterpretation, it is essential to incorporate all known geological data (e.g., vitrinite reflectance data, stratigraphic age of a sample, data obtained by other thermochronometers, etc.) into a model before the meaning of the measured ages and tT paths are evaluated. Secondly, resolution of AFT thermochronometer is limited to the temperature range of $\sim 60\text{--}120^\circ\text{C}$, therefore the parts of tT envelope defined for the zones out of this range are not necessarily representative for the real thermal evolution of a sample.

[77] The input parameters we used in this study are the following: the central FT age with 1 sigma error; track length distribution; kinetic parameter: Dpar values (apatites were etched at conditions after Donelick et al. [1999]); the end of the tT path was set to 13°C according to present-day mean surface temperature. Known geological information such as stratigraphic age of sedimentary samples or ZFT data measured on the same samples were converted into time-temperature constraints in form of boxes. The tT paths were modeled in unsupervised search style.

[78] **Acknowledgments.** This study has been funded by the German Science Foundation (DFG), project KU 1298/3. We would like to thank C. Doglioni, P. Van den haute, J. De Grave, and an anonymous reviewer whose constructive and critical comments improved the final manuscript. Gerlinde Höckh, Dorothea Mühlbayer-Renner, and Dagmar Kost (Tübingen) are gratefully acknowledged for mineral separation.

References

- Amaudric du Chaffaut, S., and P. Saliot (1979), La région de Corte: Secteur clé pour la compréhension du métamorphisme Alpin en Corse, *Bull. Soc. Geol. Fr.*, 7(21), 149–154.
- Bellaiche, G., F. Irr, and M. Labarbarie (1976), Découverte de sédiments marins fini oligocène-aquitainien au large du Massif des Maures (Canyon des Stoéchades), *C. R. Acad. Sci.*, 283, 319–322.
- Bézert, P., and R. Caby (1988), Sur l'âge post-bartonien des événements tectono-étamorphiques alpins en bordure orientale de la Corse cristalline (Nord de Corte), *Bull. Soc. Geol. Fr.*, 6, 965–971.
- Bézert, P., and R. Caby (1989), La déformation progressive de l'éocène de la région de Corte: Nouvelle données pétrostructurales et conséquences pour la tectogénèse alpine en Corse, *C. R. Acad. Sci.*, 95–101.
- Borel, G. (1995), Préalpes médianes romandes: Courbes de subsidence et implications géodynamiques, *Bull. Soc. Vaudoise Sci. Nat.*, 83(4), 293–315.
- Braun, J. (2002), Estimating exhumation rate and relief evolution by spectral analysis of age-elevation datasets, *Terra Nova*, 14, 210–214.
- Brunet, C., P. Monié, and L. Jolivet (1997), Geodynamic evolution of the Alpine Corsica based on new $^{40}\text{Ar}/^{39}\text{Ar}$ data, *Terra Abstr.*, 9, 493.
- Brunet, C., P. Monié, L. Jolivet, and J. P. Cadet (2000), Migration of compression and extension in the Tyrrhenian Sea, insights from $^{40}\text{Ar}/^{39}\text{Ar}$ ages on micas along a transect from Corsica to Tuscany, *Tectonophysics*, 321, 127–155.
- Burtner, R. L., A. Nigrini, and R. A. Donelick (1994), Thermochronology of Lower Cretaceous source rocks in the Idaho-Wyoming thrust belt, *AAPG Bull.*, 78(10), 1613–1636.
- Carmignani, L., F. A. Decandia, L. Disperati, P. L. Fantozzi, A. Lazzarotto, D. Liotta, and G. Oggiano (1995), Relationship between the Tertiary structural evolution of the Sardinia-Corsica-Provençal Domain and the northern Apennines, *Terra Nova*, 7, 128–137.
- Caron, J. M., J. R. Kienast, and C. Triboulet (1981), High-pressure-low-temperature metamorphism and polyphase alpine deformation at Sant'Andrea di cotone (eastern Corsica, France), *Tectonophysics*, 78, 419–451.
- Carpéna, J., D. Mailhé, C. W. Naeser, and G. Poupeau (1979), Sur la datation par traces de fission d'une phase tectonique d'âge Eocène supérieur en Corse, *C. R. Acad. Sci.*, 289, 829–832.
- Cavazza, W., M. Zattin, B. Ventura, and G. G. Zuffa (2001), Apatite fission-track analysis of Neogene exhumation in northern Corsica (France), *Terra Nova*, 13, 51–57.
- Chamot-Rooke, N., J. M. Gaulier, and F. Jestin (1999), Constraints on Moho depth and crustal thickness in the Liguro-Provençal basin from a 3D gravity inversion: Geodynamic implications, in *The Mediterranean Basins: Tertiary extension Within the Alpine Orogen*, edited by B. Durand et al., *Geol. Soc. Spec. Publ.*, 156, 37–61.
- Cherchi, A., and L. Montadert (1982), Oligo-Miocene rift of Sardinia and the early history of the western Mediterranean basin, *Nature*, 298, 736–739.
- Cocherie, A., P. Rossi, and L. Le Bel (1984), The Variscan calc-alkalic plutonism of western Corsica: Mineralogy and major and trace element geochemistry, *Phys. Earth Planet. Inter.*, 35, 145–178.
- Crowley, K. D., M. Cameron, and R. L. Schaeffer (1991), Experimental studies of annealing of etched fission tracks in fluorapatite, *Geochim. Cosmochim. Acta*, 55, 1449–1465.
- Daniel, J. M., L. Jolivet, B. Goffe, and C. Poinssot (1996), Crustal-scale strain partitioning: Footwall deformation below the Alpine Oligo-Miocene detachment of Corsica, *J. Struct. Geol.*, 18, 41–59.
- Danišík, M. (2005), Cooling history and relief evolution of Corsica (France) as constrained by fission track and (U-Th)/He thermochronology, Ph.D. thesis, 130 pp., University of Tübingen, Tübingen, Germany.
- Davies, J. H., and F. von Blanckenburg (1995), Slab breakoff: A model of lithosphere detachment and its test in the magmatism and deformation of collisional orogens, *Earth Planet. Sci. Lett.*, 129, 85–102.
- Dewey, J. F., M. L. Helman, E. Turco, D. H. W. Hutton, and S. D. Knott (1989), Kinematics of the western Mediterranean, in *Alpine Tectonics*, edited by M. P. Coward et al., *Geol. Soc. Spec. Publ.*, 45, 265–283.
- Doglioni, C. (1991), A proposal of kinematic modelling for W-dipping subductions: Possible applications to the Tyrrhenian-Apennines system, *Terra Nova*, 3, 423–434.
- Doglioni, C., E. Gueguen, P. Harabaglia, and F. Mongelli (1999), On the origin of west-directed subduction zones and applications to the western Mediterranean, in *The Mediterranean Basins: Tertiary Extension Within the Alpine Orogen*, edited by B. Durand et al., *Geol. Soc. Spec. Publ.*, 156, 541–570.
- Doglioni, C., E. Carminati, and E. Bonatti (2003), Rift asymmetry and continental uplift, *Tectonics*, 22(3), 1024, doi:10.1029/2002TC001459.

- Dogliani, C., F. Innocenti, C. Morellato, D. Procaccianti, and D. Scrocca (2004), On the Tyrrhenian sea opening, *Mem. Descr. Carta Geol. Ital.*, **64**, 147–164.
- Donelick, R. A., R. A. Ketcham, and W. D. Carlson (1999), Variability of apatite fission-track annealing kinetics: II. Crystallographic orientation effects, *Am. Mineral.*, **84**(9), 1224–1234.
- Dumitru, T. A. (1993), A new computer-automated microscope stage system for fission-track analysis, *Nucl. Tracks Radiat. Meas.*, **21**, 575–580.
- Dunkl, I. (2002), TRACKKEY: A Windows program for calculation and graphical presentation of fission track data, *Comput. Geosci.*, **28**(2), 3–12.
- Dunkl, I., W. Frisch, and J. Kuhlemann (1999), Fission track record of the thermal evolution of the eastern Alps: Review of the main zircon age clusters and the significance of the 160 Ma event, 4th Workshop on Alpine Geological Studies, Tübingen, Germany, *Tübinger Geowiss. Arb., Reihe A*, **52**, 77–78.
- Durand-Delga, M. (1978), *Cors-Guides Géologiques Régionaux*, 208 pp, Masson, Paris.
- Durand-Delga, M. (1984), Principaux trait de la Corse Alpine et corrélation avec les Alpes ligures, *Mem. Soc. Geol. Ital.*, **28**, 285–329.
- Egal, E. (1992), Structures and tectonic evolution of the external zone of Alpine Corsica, *J. Struct. Geol.*, **14**(10), 1215–1228.
- Fellin, M. G. (2003), Neogene to Quaternary thermo-tectonic evolution of north-eastern Corsica (France), Ph.D. thesis, 90 pp., Univ. of Bologna, Bologna, Italy.
- Fellin, M. G., V. Picotti, and M. Zattin (2005a), Neogene to Quaternary multiple rifting and inversion in northeastern Corsica: Retreat and collision in the western Mediterranean, *Tectonics*, **24**, TC1011, doi:10.1029/2003TC001613.
- Fellin, M. G., M. Zattin, V. Picotti, P. W. Reiners, and S. Nicolescu (2005b), Relief evolution in northern Corsica (western Mediterranean): Constraints on uplift and erosion on long-term and short-term timescales, *J. Geophys. Res.*, **110**, F01016, doi:10.1029/2004JF000167.
- Ferrandini, L., P. Rossi, M. Ferrandini, G. Farjanel, L. Ginsburg, M. Schuler, and F. Geissert (1999), La Formation conglomératique du Vazzio près d' Ajaccio (Corse-du-Sud), un témoin des dépôts du Châtien supérieur continental synrift en méditerranée occidentale, *C. R. Acad. Sci., Ser. II*, **329**(4), 271–278.
- Ferrandini, M., J. Ferrandini, M. D. Loÿe-Pilot, J. Butterlin, J. Cravatte, and M. C. Janin (1998), Le Miocène du bassin de Saint-Florent (Corse): Modalités de la transgression du Burdigalien supérieur et mise en évidence du Serravallien, *Geobios*, **31**(1), 125–137.
- Fournier, M., L. Jolivet, and B. Goffé (1991), Alpine Corsica metamorphic core complex, *Tectonics*, **10**, 1173–1186.
- Frisch, W. (1979), Tectonic progradation and plate tectonic evolution of the Alps, *Tectonophysics*, **60**, 121–139.
- Frisch, W. (1981), Plate motions in the Alpine region and their correlation to the opening of the Atlantic Ocean, *Geol. Rundsch.*, **70**, 402–411.
- Galbraith, R. F., and G. M. Laslett (1993), Statistical models for mixed fission track ages, *Nucl. Tracks Radiat. Meas.*, **21**, 459–470.
- Gallagher, K., and R. W. Brown (1997), The onshore record of passive margin evolution, *J. Geol. Soc. London*, **154**, 451–457.
- Gallagher, K., R. Brown, and C. Johnson (1998), Fission track analysis and its applications to geological problems, *Annu. Rev. Earth Planet. Sci.*, **26**, 519–572.
- Gibbons, W., and J. Horák (1984), Alpine metamorphism of Hercynian hornblende granodiorite beneath the blueschists facies Schistes Lustrés nappe of NE Corsica, *J. Metamorph. Geol.*, **2**, 95–113.
- Gleadow, A. J. W. (1981), Fission track dating methods: What are the real alternatives?, *Nucl. Tracks Radiat. Meas.*, **5**, 3–14.
- Gleadow, A. J. W., I. R. Duddy, and P. F. Green (1986a), Fission track lengths in the apatite annealing zone and the interpretation of mixed ages, *Earth Planet. Sci. Lett.*, **78**, 245–254.
- Gleadow, A. J. W., I. R. Duddy, and P. F. Green (1986b), Confined fission track lengths in apatite: A diagnostic tool for thermal history analysis, *Contrib. Mineral. Petrol.*, **94**, 405–415.
- Gorini, C., A. Le Marrec, and A. Mauffret (1993), Contribution to the structural and sedimentary history of the Gulf of Lions (western Mediterranean) from ECORS profiles, industrial seismic profiles and well data, *Bull. Soc. Geol. Fr.*, **164**, 353–363.
- Gueguen, E., C. Dogliani, and M. Fernandez (1998), On the post-25 Ma geodynamic evolution of the western Mediterranean, *Tectonophysics*, **298**, 259–269.
- Hurford, A. J. (1998), ZETA: The ultimate solution to fission-track analysis calibration or just an interim measure, in *Advances in Fission-Track Geochronology*, edited by P. Van den haute and F. De Corte, pp. 19–32, Springer, New York.
- Hurford, A. J., and P. F. Green (1982), A user's guide to fission-track dating calibration, *Earth Planet. Sci. Lett.*, **59**, 343–354.
- Hurford, A. J., and P. F. Green (1983), The zeta age calibration of fission-track dating, *Chem. Geol.*, **41**, 285–312.
- Jakni, B. (2000), Thermochronologie par traces de fission des marges conjuguées du bassin Liguro-Provençal: La Corse et le massif des Maures-Tanneron, Ph.D. thesis, 344 pp., Univ. Joseph Fourier, Grenoble, France.
- Jakni, B., G. Poupeau, M. Sosson, P. Rossi, J. Ferrandini, and P. Guennoc (2000), Dénudations cénozoïques en Corse: Une analyse thermo-chronologique par traces de fission sur apatites, *C. R. Acad. Sci.*, **331**, 775–782.
- Jolivet, L., and C. Faccenna (2000), Mediterranean extension and the Africa-Eurasia collision, *Tectonics*, **19**, 1095–1106.
- Jolivet, L., R. Dubois, M. Fournier, B. Goffé, A. Michard, and C. Jourdan (1990), Ductile extension in Alpine Corsica, *Geology*, **18**, 1007–1010.
- Jolivet, L., J. M. Daniel, and M. Fournier (1991), Geometry and kinematics of ductile extension in Alpine Corsica, *Earth Planet. Sci. Lett.*, **104**, 278–291.
- Jolivet, L., et al. (1998), Midcrustal shear zones in post-orogenic extension: Example from the Tyrrhenian Sea, *J. Geophys. Res.*, **103**, 12,123–12,160.
- Jourdan, C. (1988), Balagne orientale et massif du Tende (Corse septentrionale): Etude structurale, interprétation des accidents et des déformations, reconstitutions géodynamiques, Ph.D. thesis, Univ. de Paris Sud, Orsay, France.
- Ketcham, R. A. (2005), Forward and inverse modeling of low-temperature thermochronometry data, in *Low-Temperature Thermochronology: Techniques, Interpretations, and Applications*, *Rev. Mineral. Geochem.*, vol. 58, edited by P. W. Reiners and T. A. Ehlers, pp. 275–314, Am. Mineral. Soc., Washington, D. C.
- Ketcham, R. A., R. A. Donelick, and W. D. Carlson (1999), Variability of apatite fission-track annealing kinetics: III. Extrapolation to geologic time scales, *Am. Mineral.*, **84**, 1235–1255.
- Lahondère, D. (1988), Le métamorphisme éclogitique dans les orthogneiss, et les metabasites ophiolitiques de la région de Farinole (Corse), *Bull. Soc. Geol. Fr.*, **4**, 579–585.
- Lahondère, D. (1991), Les schistes bleus et les éclogites à lawsonite des unités continentales et océaniques de la Corse alpine: Nouvelles données pétrologiques et structurales, thesis, Univ. Montpellier, France.
- Lahondère, D., and C. Guerrot (1997), Datation Nd-Sm du métamorphisme éclogitique en Corse alpine: Un argument pour l'existence, au Crétacé supérieur, d'une zone de subduction active localisée le long du bloc corso-sarde, *Geol. Fr.*, **3**, 3–11.
- Loup, B. (1992), Mesozoic subsidence and stretching models of the lithosphere in Switzerland (Jura, Swiss Plateau and Helvetic realm), *Ecologe Geol. Helv.*, **85**(3), 541–572.
- Lucazeau, F., and D. Mailhé (1986), Heat flow, heat production and fission track data from the Hercynian basement around the Provençal Basin (western Mediterranean), *Tectonophysics*, **128**, 335–356.
- Mailhé, D. (1982), Application des méthodes de datation ⁴⁰Ar-³⁹Ar et traces de fission de l'uranium à l'étude du déroulement de l'orgénèse alpine en Corse, thesis, Univ. Montpellier, Montpellier, France.
- Mailhé, D., F. Lucazeau, and G. Vasseur (1986), Uplift history of thrust belts: An approach based on fission track data and thermal modelization, *Tectonophysics*, **124**, 177–191.
- Malavieille, J. (1983), Étude tectonique et microtectonique de la nappe de socle de Centuri (zone des Schistes Lustrés de Corse), Conséquence pour la géométrie de la chaîne alpine, *Bull. Soc. Geol. Fr.*, **25**, 195–204.
- Malavieille, J., A. Chemenda, and C. Larroque (1998), Evolutionary model for Alpine Corsica: Mechanism for ophiolite emplacement and exhumation of high pressure rocks, *Terra Nova*, **10**, 317–322.
- Maluski, H. (1977), Application de la méthode ⁴⁰Ar-³⁹Ar aux minéraux des roches cristallines perturbées par des événements thermiques et tectoniques en Corse, *Bull. Soc. Geol. Fr.*, **19**(4), 849–855.
- Mancktelow, N. S., and B. Grasemann (1997), Time-dependent effects of heat advection and topography on cooling histories during erosion, *Tectonophysics*, **270**, 167–195.
- Mattauer, M., M. Faure, and J. Malavieille (1981), Transverse lineation and large scale structures related to Alpine obduction in Corsica, *J. Struct. Geol.*, **3**, 401–409.
- Naeser, N. D. (1992), Miocene cooling in the south-western Powder River Basin, Wyoming - Preliminary evidence from apatite fission-track analysis, *U. S. Geol. Surv. Bull.*, **1917-O**, 17 pp.
- Nardi, R., A. Puccinelli, and M. Verani (1978), Carta geologica della Balagne "sedimentaria" (Corsica) alla scala 1:25.000 e note illustrative, *Bull. Soc. Geol. Ital.*, **97**, 11–30.
- Orszag-Sperber, F., and M.-D. Pilot (1976), Grands traits du Néogène de Corse, *Bull. Soc. Geol. Fr.*, **18**(5), 1183–1187.
- Réhault, J.-P., G. Boillot, and A. Mauffret (1984), The western Mediterranean basin geological evolution, *Mar. Geol.*, **55**, 447–477.
- Rollet, N., J. Déverchère, M. O. Beslier, P. Guennoc, J. P. Réhault, M. Sosson, and C. Truffert (2002), Back arc extension, tectonic inheritance, and volcanism in the Ligurian Sea, western Mediterranean, *Tectonics*, **21**(3), 1015, doi:10.1029/2001TC900027.
- Rosenbaum, G., K. Regenauer-Lieb, and R. Weinberg (2005), Continental extension: From core complexes to rigid block faulting, *Geology*, **33**, 609–612.
- Rossi, P., and A. Cocherie (1991), Genesis of a Variscan batholith: Field, petrological and mineralogical evidence from Corsica-Sardinia batholith, *Tectonophysics*, **195**, 319–346.
- Rossi, P., J. Rouire, and M. Durand-Delga (1980), Carte géologique de la France, A 1/250,000, Corse, sheet 44/45, Notice explicative de la feuille, 80 pp., Bur. Rech. Geol. Miner., Orléans, France.
- Sérrane, M. (1999), The Gulf of Lion continental margin (NW Mediterranean) revisited by IBS: An overview, in *The Mediterranean Basins: Tertiary Extension Within the Alpine Orogen*, edited by B. Durand et al., *Geol. Soc. Spec. Publ.*, **156**, 15–36.
- Stüwe, K., and M. Hintermüller (2000), Topography and isotherms revisited: The influence of laterally migrating drainage divides, *Earth Planet. Sci. Lett.*, **184**, 287–303.
- Stüwe, K., L. White, and R. W. Brown (1994), The influence of eroding topography on steady-state isotherms: Application to fission track analysis, *Earth Planet. Sci. Lett.*, **124**, 63–74.
- Turcotte, D. L., and G. Schubert (2002), *Geodynamics*, 2nd ed., 456 pp., Cambridge Univ. Press, New York.

- Vance, J. (1999), Zircon fission track evidence for a Jurassic (Tethyan) thermal event in the western Alps, *Mem. Sci. Geol. Padova*, 51(2), 473–476.
- Van der Voo, R. (1993), *Paleomagnetism of the Atlantic, Tethys and Iapetus Oceans*, 411 pp. Cambridge Univ. Press, New York.
- Vigliotti, L., and D. V. Kent (1990), Paleomagnetic results of Tertiary sediments from Corsica: Evidence of post-Eocene rotation, *Phys. Earth Planet. Inter.*, 62, 97–108.
- Vigliotti, L., and V. E. Langenheim (1995), When did Sardinia stop rotating? New paleomagnetic results, *Terra Nova*, 7, 424–435.
- Vigliotti, L., W. Alvarez, and M. McWilliams (1990), No relative motion detected between Corsica and Sardinia, *Earth Planet. Sci. Lett.*, 98, 313–318.
- Wagner, G. A. (1968), Fission track dating of apatites, *Earth Planet. Sci. Lett.*, 4, 411–415.
- Wagner, G. A., and G. M. Reimer (1972), Fission track tectonics: The tectonic interpretation of fission track apatite ages, *Earth Planet. Sci. Lett.*, 14, 263–268.
- Wagner, G. A., and P. Van den haute (1992), *Fission-Track Dating*, 285 pp., Enke, Stuttgart, Germany.
- Wagner, G. A., G. M. Reimer, and E. Jäger (1977), Cooling ages derived by apatite fission-track, mica Rb-Sr and K-Ar dating: The uplift and cooling history of the central Alps, *Mem. Inst. Geol. Miner. Univ. Padova*, 30, 1–27.
- Warburton, J. (1986), The ophiolite-bearing Schistes Lustrés Nappe in Alpine Corsica: A model for the emplacement of ophiolites that have suffered HP/LT metamorphism, *Mem. Geol. Soc. Am.*, 164, 313–331.
- Yamada, R., T. Tagami, S. Nishimura, and H. Ito (1995), Annealing kinetics of fission tracks in zircon: An experimental study, *Chem. Geol.*, 122, 249–258.
- Zarki-Jakni, B., P. Van der Beek, G. Poupeau, M. Sosson, E. Labrin, P. Rossi, and J. Ferrandini (2004), Cenozoic denudation of Corsica in response to Ligurian and Tyrrhenian extension: Results from apatite fission-track thermochronology, *Tectonics*, 23, TC1003, doi:10.1029/2003TC001535.
- Zattin, M., M. G. Fellin, W. Cavazza, V. Picotti, J. A. Vance, and G. G. Zuffa (2001), Exhumation of northern Corsica (France), *Geophys. Res. Abstr.*, 3, 531.
- Zaun, P., and G. A. Wagner (1985), Fission track stability in zircon under geological conditions, *Nucl. Tracks Radiat. Meas.*, 10, 303–307.
- Zeck, H. P. (1999), Alpine plate kinematics in the western Mediterranean: A westward-directed subduction regime followed by slab roll-back and slab detachment, in *The Mediterranean Basins: Tertiary Extension Within the Alpine Orogen*, edited by B. Durand et al., *Geol. Soc. Spec. Publ.*, 156, 109–120.

M. Danišík, W. Frisch, J. Kuhlemann, and B. Székely, Institute of Geosciences, University of Tübingen, Sigwartstrasse 10, D-72076 Tübingen, Germany. (martin.danisik@uni-tuebingen.de; frisch@uni-tuebingen.de; kuhlemann@uni-tuebingen.de; balazs.szekely@uni-tuebingen.de)

I. Dunkl, Geoscience Center Göttingen, Sedimentology and Environmental Geology, Goldschmidtstrasse 3, D-37077 Göttingen, Germany. (istvan.dunkl@geo.uni-goettingen.de)